Supporting Information

How does chiral self-sorting take place in the formation of homochiral Pd_6L_8 capsules consisting of cyclotriveratrylene-based chiral tritopic ligands?

Shumpei Kai,[a] Tatsuo Kojima,[a] Flora L. Thorp-Greenwood,[b] Michaele J. Hardie,[b] and Shuichi Hiraoka*,[a]

[a]*Department of Basic Science, Graduate School of Arts and Sciences, The University of Tokyo 3-8-1 Komaba, Meguro-ku, Tokyo 153-8902, Japan*

[b]*School of Chemistry, University of Leeds, Woodhouse Lane, Leeds, LS2 9JT, UK*

E-mail: chiraoka@mail.ecc.u-tokyo.ac.jp

Contents

General information

^{1}H NMR spectra were recorded using a Bruker AV-500 (500 MHz) spectrometer. All ^{1}H spectra were referenced using a residual solvent peak, CD_3NO_2 (δ 4.33) and $CDCl_3$ (δ 7.26). Electrospray ionization time-of-flight (ESI-TOF) mass spectra were obtained using a Waters Xevo G2-S Tof mass spectrometer.

Materials

Unless otherwise noted, all solvents and reagents were obtained from commercial suppliers (TCI Co., Ltd., WAKO Pure Chemical Industries Ltd., KANTO Chemical Co., Inc., and Sigma-Aldrich Co.) and were used as received. Tritopic ligand **1** was prepared according to the literature.[1] Enantiomers of **1** were resolved by chiral HPLC (CHIRALPAK OD-H (ODH0CE-RA010), 0.46 cm × 25 cm, MeCN/MeOH = 80/20 (v/v), 1.0 ml/min, 280 nm).[2]

Procedure for Monitoring the Self-Assembly Process of the $Pd_6\mathbf{1}_8(OTf)_{12}$ Capsule

Self-assembly of the $Pd_6\mathbf{1}^*_8(OTf)_{12}$ capsule from **1*** and $PdPy^*_4(OTf)_2$

A 2.4 mM solution of [2.2]paracyclophane in $CHCl_3$ (125 µL), which was used as an internal standard, was added to two NMR tubes (tubes **I** and **II**) and the solvent was removed in vacuo. A solution of $PdPy^*_4(OTf)_2$ (18 mM) in CD_3NO_2 was prepared (solution **A**). Solution **A** (50 µL) and CD_3NO_2 (450 µL) were added in tube **I**. The exact concentration of $PdPy^*_4(OTf)_2$ in solution **A** was determined through the comparison of the signal intensity with [2.2]paracyclophane by ^{1}H NMR. A 12 mM solution of tritopic ligand **1*** in $CHCl_3$ (100 µL) was added to tube **II** and the solvent was removed in vacuo. Then CD_2Cl_2 (110 µL) and CD_3NO_2 (390 µL) were added and the exact amount of **1*** in tube **II** was determined through the comparison of the signal intensity with [2.2]paracyclophane by ^{1}H NMR. 0.75 eq. (against the amount of ligand **1*** in tube **II**) of $PdPy^*_4(OTf)_2$ in solution **A** (*ca.*50 µL; the exact amount was determined based on the exact concentration of solution **A**) was added into tube **II** at 263 K and then the self-assembly of the $Pd_6\mathbf{1}^*_8(OTf)_{12}$ capsule was monitored at 298 K by ^{1}H NMR spectroscopy. The exact ratio of **1*** and $PdPy^*_4(OTf)_2$ was unambiguously determined by the comparison of the integral of each ^{1}H signal of [2.2]paracyclophane. The quantities of **1***, $[PdPy^*_4]^{2+}$, the $Pd_6\mathbf{1}_8$ capsule, and Py* were quantified by the integral of each ^{1}H signal against the signal of the internal standard ([2.2]paracyclophane). In order to confirm the reproducibility of the measurements, the same experiments were carried out three times (runs 1–3). Selected ^{1}H NMR spectra of run 1 are shown in Figure 2a. The existence ratios of **1***, $PdPy^*_4(OTf)_2$, $Pd_6\mathbf{1}^*_8$, Py*, and all the intermediates (**Int**) for each run are listed in Tables S1–S4 and the average values with standard error obtained from the three runs are shown in Figures 3a, 3b, and 3e. The ($\langle n \rangle, \langle k \rangle$) plots obtained from three runs are shown in Figure 4b and 4b.

Self-assembly of the $Pd_6\mathbf{1}_8(OTf)_{12}$ capsule from a racemic mixture of **1** and $PdPy^*_4(OTf)_2$

The self-assembly of the $Pd_6\mathbf{1}_8(OTf)_{12}$ capsule from a racemic mixture of **1** and $PdPy^*_4(OTf)_2$ was carried out in the same way as from **1*** and $PdPy^*_4(OTf)_2$. Selected ^{1}H NMR spectra of run 1 are shown in Figure 2b. The existence ratios of **1**, $PdPy^*_4(OTf)_2$, $Pd_6\mathbf{1}_8$, Py*, and all the intermediates (**Int**) for each run are listed in Tables S5–S8 and the average values with standard error obtained from the three runs are shown in Figures 3c, 3d, and 3f. The ($\langle n \rangle, \langle k \rangle$) plots obtained from three runs are shown in Figure 4c and 4d.

Self-assembly of the $Pd_6\mathbf{1}_8(OTf)_{12}$ capsule from **1*** and $Pd(CH_3CN)_4(OTf)_2$

A 2.4 mM solution of [2.2]paracyclophane in $CHCl_3$ (125 µL), which was used as an internal standard, and a 12 mM solution of tritopic ligand **1*** in $CHCl_3$ (100 µL) were added to an NMR tube and the solvent was removed in vacuo (tube **I**). Then the solvent (CD_2Cl_2 (110 µL) and CD_3NO_2 (390 µL) or DMSO-d_6 (500 μL)) was added and the exact amount of **1*** in tube **I** was determined based on the intensity of the signal of [2.2]paracyclophane by ^{1}H NMR spectroscopy. A solution of $Pd(CH_3CN)_4(OTf)_2$ (18 mM) in CD_3NO_2 was prepared (solution **A**). 0.75 eq. (against the amount of ligand **1*** in tube **I**) of $Pd(CH_3CN)_4(OTf)_2$ in solution **A** (*ca.* 50 μL) was added into tube **I** at 263 K and then the self-assembly of the Pd_6**1***$_8(OTf)_{12}$ capsule was monitored at 298 K by ^{1}H NMR spectroscopy. The quantities of **1*** and the Pd_6**1***$_8$ capsule were quantified by the integral of each ^{1}H signal against the signal of the internal standard ([2.2]paracyclophane). Selected ^{1}H NMR spectra in CD_3NO_2 and CD_2Cl_2 (v/v = 4/1) and in DMSO-d_6 are shown in Figure S1a and S1b, respectively.

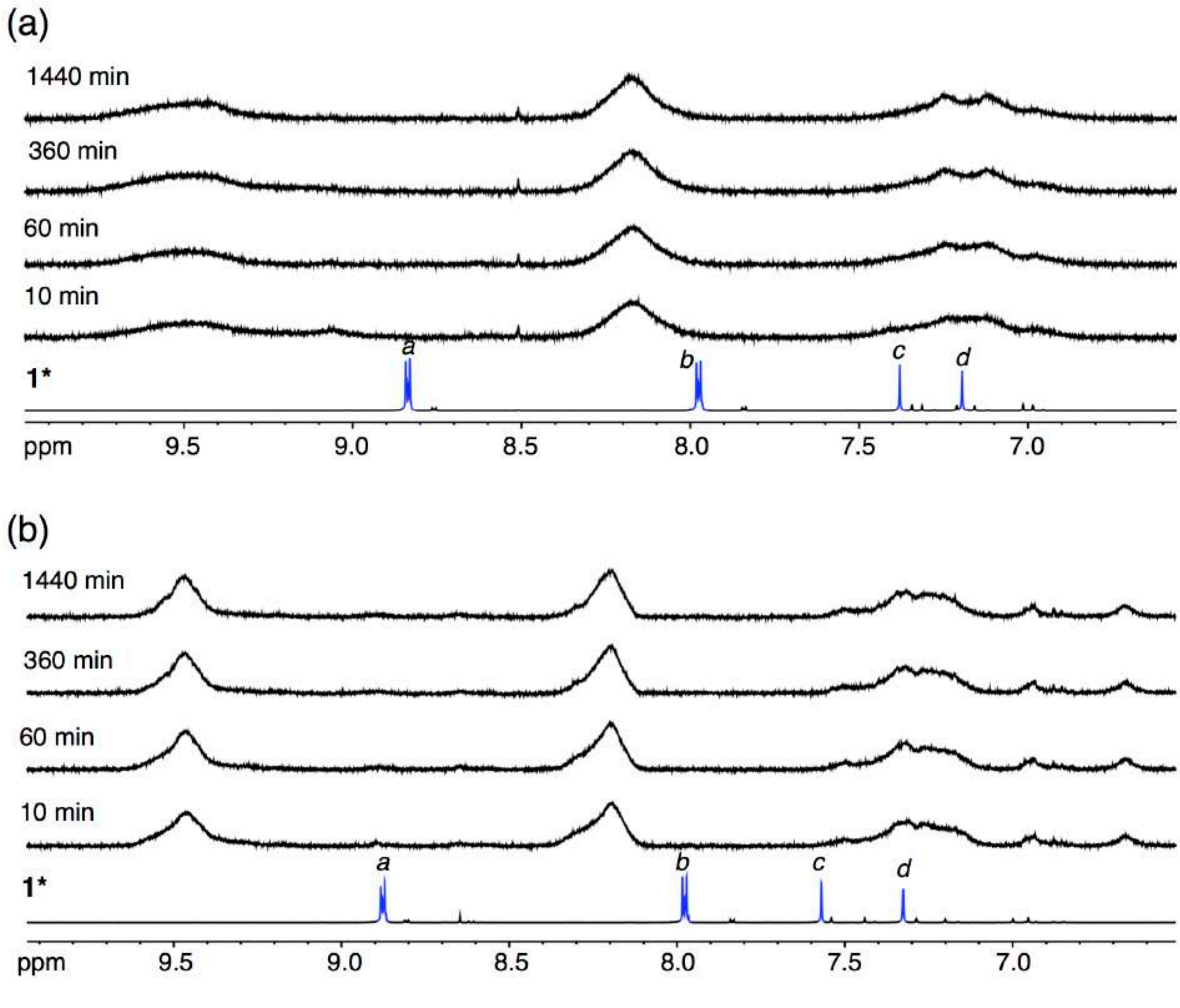

Figure S1. Partial ^{1}H NMR (500 MHz, aromatic region, 298 K) of the self-assembly of the Pd_6**1***$_8(OTf)_{12}$ capsule from **1*** and $Pd(CH_3CN)_4(OTf)_2$ (a) in CD_3NO_2 and CD_2Cl_2 (v/v = 4/1) and (b) in DMSO-d_6.

Determination of the Existence Ratio of Each Species

The relative integral value of each [1]H NMR signal against the internal standard [2.2]paracyclophane is used as the integral value in this description. We define the integral values of the signal for the substrates and the products, at each time t as follows:

$I_L(t)$: the integral value of the *d* proton in free ligand **1**
$I_M(t)$: the integral value of the proton at the *e* proton of Py* in $[PdPy*_4]^{2+}$
$I_{capsule}(t)$: the integral value of the *d* proton in the Pd_6**1**$_8$ capsule
$I_{Py*}(t)$: the integral value of the proton at the *e* proton of free Py*

$I_M(0)$ was determined based on the exact concentration of solution **A** determined by [1]H NMR and the exact volume of the solution **A** added into tube **II**.
$I_L(0)$ was determined based on [1]H NMR measurement before the addition of solution **A** into tube **II**.

Existence ratio of $[PdPy*_4]^{2+}$
As the total amount of $[PdPy*_4]^{2+}$ corresponds to $I_M(0)$, the existence ratio of $[PdPy*_4]^{2+}$ at t is expressed by $I_M(t)/I_M(0)$.

Existence ratio of **1**
As the total amount of free ligand **1** corresponds to $I_L(0)$, the existence ratio of **1** at t is expressed by $I_L(t)/I_L(0)$.

Existence ratio of Py*
As the total amount of Py* corresponds to $I_M(0)$, the existence ratio of Py* at t is expressed by $I_{Py*}(t)/I_M(0)$.

Existence ratio of the Pd_6**1**$_8$ capsule
As the Pd_6**1**$_8$ capsule is quantified based on **1**, the existence ratio of the capsule at t is expressed by $I_{capsule}(t)/I_L(0)$.

Existence ratio of the total intermediates
The existence ratio of the total intermediates is determined based on the amount of ligand **1** in the intermediates. Thus the existence ratio of the total intermediate is calculated by subtracting the other species containing **1** (free **1** and the Pd_6**1**$_8$ capsule) from the total amount of **1** ($I_L(0)$). The existence ratio of the total intermediates at t is expressed by $(I_L(0) - I_L(t) - I_{capsule}(t))/I_L(0)$.

⟨*a*⟩
The total amount of Pd(II) ion corresponds to $I_M(0)/4$. The amount of Pd(II) ion in $[PdPy*_4]^{2+}$ at t corresponds to $I_M(t)/4$. The amount of Pd(II) ion in the Pd_6**1**$_8$ capsule at t corresponds to $I_{capsule}(t) \times 3/4$.. The amount of Pd(II) ion in the intermediates at t is thus expressed by $I_M(0)/4 - I_M(t)/4 - I_{capsule}(t) \times 3/4$.

⟨*b*⟩
The total amount of ligand **1** corresponds to $I_L(0)$. The amount of free ligand **1** at t corresponds to $I_L(t)$. The amount of ligand **1** in the Pd_6**1**$_8$ capsule at t corresponds to $I_{capsule}(t)$. The amount of ligand **1** in the intermediates at t is thus expressed by $I_L(0) - I_L(t) - I_{capsule}(t)$.

$\langle c \rangle$

The total amount of Py* corresponds to $I_M(0)$. The amount of free Py* at t corresponds to $I_{Py*}(t)$. The amount of Py* in $[PdPy*_4]^{2+}$ at t corresponds to $I_M(t)$. The amount of Py* in the intermediates at t is thus expressed by $I_M(0) - I_{Py*}(t) - I_M(t)$.

The $\langle n \rangle$ and $\langle k \rangle$ values are determined from $\langle a \rangle$, $\langle b \rangle$, and $\langle c \rangle$ values by eqs. (1) and (2).

$$\langle n \rangle = \frac{4\langle a \rangle - \langle c \rangle}{\langle b \rangle} \quad (1)$$

$$\langle k \rangle = \frac{\langle a \rangle}{\langle b \rangle} \quad (2)$$

Table S1. Time variation of **1***, $PdPy^*_4(OTf)_2$, Py*, Pd_6**1***$_8(OTf)_{12}$, and **Int** and the ($\langle n \rangle$, $\langle k \rangle$) values for the self-assembly of the Pd_6**1***$_8(OTf)_{12}$ capsule from **1*** and $PdPy^*_4(OTf)_2$ in CD_3NO_2/CD_2Cl_2 (v/v = 4/1) at 298 K ([**1***]$_0$ = 2.2 mM).

Time (min)	$[PdPy^*_4]^{2+}$ (%)	**1*** (%)	$[Pd_6$**1***$_8]^{12+}$ (%)	Py* (%)	**Int** (%)	$[PdPy^*_4]^{2+}$ SE	**1*** SE	$[Pd_6$**1***$_8]^{12+}$ SE	Py* SE	**Int** SE
0	100	100	0	0	0	0	0	0	0	0
5	31.2	16.7	12.2	44.3	71.1	1.04	0.79	0.20	1.28	0.98
10	18.6	11.5	15.1	58.9	73.4	0.96	1.53	0.31	1.28	1.24
15	11.1	9.4	20.9	68.1	69.8	0.51	0.61	0.90	0.93	1.40
20	8.6	8.6	25.9	73.8	65.5	0.14	0.71	1.40	1.93	1.69
25	7.5	8.1	28.2	77.9	63.6	0.27	0.64	1.17	2.33	1.34
30	6.6	7.4	30.2	80.3	62.3	0.21	0.36	1.03	2.29	0.87
35	5.9	7.1	32.1	82.5	60.8	0.14	0.40	0.77	1.82	0.49
40	5.3	6.5	34.0	84.1	59.5	0.17	0.20	1.09	1.10	0.91
45	5.2	6.2	35.0	84.5	58.9	0.21	0.18	1.35	1.03	1.23
50	4.6	5.9	36.7	85.6	57.4	0.03	0.15	1.07	0.88	1.07
55	4.5	5.7	37.5	86.6	56.8	0.06	0.20	1.60	0.29	1.69
60	4.4	5.1	38.9	87.3	56.0	0.03	0.45	1.78	0.57	1.65
75	4.2	4.9	40.3	87.9	54.9	0.06	0.45	1.22	0.36	1.05
90	4.1	4.7	41.7	88.5	53.6	0.09	0.44	0.85	0.30	0.53
105	4.0	4.6	42.9	88.9	52.5	0.12	0.39	0.65	0.32	0.28
120	3.7	4.4	44.0	89.4	51.6	0.15	0.35	0.71	0.52	0.66
180	3.4	4.0	46.9	90.0	49.1	0.29	0.29	0.35	0.43	0.11
240	3.4	3.7	49.4	90.7	46.9	0.29	0.28	0.81	0.15	0.57
300	3.3	3.5	50.6	90.9	45.9	0.24	0.25	0.54	0.26	0.59
360	3.3	3.4	52.6	91.3	44.0	0.22	0.18	1.04	0.20	1.09
420	3.3	3.3	53.2	91.7	43.6	0.22	0.18	1.20	0.39	1.33
480	3.2	3.2	53.9	92.1	42.9	0.24	0.17	1.04	0.47	1.15
540	3.1	3.1	54.6	92.6	42.3	0.24	0.18	0.69	0.50	0.82
720	3.1	3.0	56.0	93.0	41.0	0.23	0.28	0.76	0.68	1.04
1440	3.0	3.0	58.8	93.2	38.3	0.32	0.27	0.97	0.75	1.17

*SE = Standard error.

Time (min)	$\langle n \rangle$	$\langle k \rangle$	$\langle n \rangle$ SE	$\langle k \rangle$ SE
5	1.35	0.598	0.056	0.017
10	1.79	0.678	0.090	0.006
15	2.03	0.732	0.041	0.012
20	2.20	0.750	0.102	0.007
25	2.35	0.758	0.133	0.006
30	2.41	0.760	0.125	0.002
35	2.48	0.765	0.112	0.005
40	2.53	0.765	0.065	0.004
45	2.52	0.762	0.055	0.004
50	2.55	0.767	0.056	0.002
55	2.59	0.767	0.023	0.003
60	2.59	0.759	0.045	0.006
75	2.60	0.759	0.028	0.006
90	2.62	0.758	0.011	0.006
105	2.63	0.758	0.009	0.006
120	2.64	0.760	0.020	0.004
180	2.63	0.758	0.010	0.005
240	2.64	0.755	0.016	0.004
300	2.64	0.753	0.008	0.003
360	2.64	0.752	0.012	0.001
420	2.65	0.750	0.019	0.002
480	2.67	0.751	0.026	0.002
540	2.70	0.750	0.033	0.002
720	2.70	0.748	0.052	0.001
1440	2.70	0.749	0.049	0.001

Table S2. Time variation of **1***, PdPy*$_4$(OTf)$_2$, Py*, Pd$_6$**1***$_8$(OTf)$_{12}$, and **Int** and $\langle a \rangle$–$\langle c \rangle$ of the average composition of **Int**, Pd$_{\langle a \rangle}$**1***$_{\langle b \rangle}$Py*$_{\langle c \rangle}$, and the ($\langle n \rangle$, $\langle k \rangle$) values for the self-assembly of the Pd$_6$**1***$_8$(OTf)$_{12}$ capsule from **1*** and PdPy*$_4$(OTf)$_2$ in CD_3NO_2/CD_2Cl_2 (v/v = 4/1) at 298 K ([**1***]$_0$ = 2.2 mM) (run 1).

Time (min)	[PdPy*$_4$]$^{2+}$ (%)	**1*** (%)	[Pd$_6$**1***$_8$]$^{12+}$ (%)	Py* (%)	**Int** (%)	$\langle a \rangle$	$\langle b \rangle$	$\langle c \rangle$	$\langle n \rangle$	$\langle k \rangle$
0	100	100	0	0	0	–	–	–	–	–
5	29.1	18.3	12.6	44.9	69.1	0.187	0.296	0.333	1.40	0.632
10	17.7	9.3	15.4	58.7	75.4	0.215	0.323	0.303	1.73	0.666
15	11.9	8.3	20.4	67.8	71.3	0.217	0.305	0.260	2.00	0.712
20	8.4	7.5	27.2	72.6	65.3	0.207	0.280	0.244	2.09	0.740
25	6.9	7.2	29.7	75.5	63.1	0.203	0.270	0.226	2.17	0.752
30	6.3	6.8	32.1	78.0	61.1	0.198	0.262	0.202	2.25	0.756
35	5.8	6.4	33.6	79.5	60.0	0.195	0.257	0.189	2.30	0.757
40	5.5	6.1	36.1	82.9	57.8	0.188	0.247	0.148	2.43	0.758
45	5.5	5.9	37.7	84.0	56.4	0.183	0.242	0.135	2.46	0.755
50	4.6	5.8	38.5	84.0	55.7	0.183	0.239	0.146	2.45	0.766
55	4.6	5.6	39.9	86.2	54.5	0.178	0.233	0.118	2.55	0.764
60	4.4	4.2	41.3	87.2	54.5	0.174	0.233	0.108	2.53	0.747
75	4.3	4.0	42.1	88.1	53.9	0.172	0.231	0.098	2.56	0.746
90	4.1	3.9	43.3	89.0	52.8	0.169	0.226	0.087	2.60	0.746
105	4.0	3.8	44.2	89.5	51.9	0.166	0.222	0.083	2.62	0.747
120	3.5	3.7	44.7	90.3	51.6	0.166	0.221	0.080	2.65	0.753
180	3.0	3.5	47.6	90.6	48.9	0.159	0.209	0.082	2.64	0.758
240	2.9	3.2	50.6	90.8	46.2	0.149	0.198	0.081	2.61	0.754
300	2.9	3.0	50.5	91.3	46.4	0.150	0.199	0.075	2.63	0.752
360	2.9	3.1	52.9	91.4	44.0	0.142	0.189	0.074	2.62	0.753
420	2.9	3.0	53.4	92.4	43.6	0.140	0.187	0.060	2.69	0.753
480	2.7	3.0	54.3	92.7	42.7	0.138	0.183	0.059	2.70	0.755
540	2.7	2.9	54.4	93.1	42.7	0.138	0.183	0.055	2.71	0.753
720	2.6	2.4	54.6	93.4	43.0	0.138	0.184	0.051	2.71	0.746
1440	2.4	2.4	57.8	94.0	39.8	0.128	0.170	0.046	2.73	0.752

Table S3. Time variation of **1***, PdPy*$_4$(OTf)$_2$, Py*, Pd$_6$**1***$_8$(OTf)$_{12}$, and **Int** and $\langle a\rangle$–$\langle c\rangle$ of the average composition of **Int**, Pd$_{\langle a\rangle}$**1***$_{\langle b\rangle}$Py*$_{\langle c\rangle}$, and the ($\langle n\rangle$, $\langle k\rangle$) values for the self-assembly of the Pd$_6$**1***$_8$(OTf)$_{12}$ capsule from **1*** and PdPy*$_4$(OTf)$_2$ in CD_3NO_2/CD_2Cl_2 (v/v = 4/1) at 298 K ([**1***]$_0$ = 2.2 mM) (run 2).

Time (min)	[PdPy*$_4$]$^{2+}$ (%)	**1*** (%)	[Pd$_6$**1***$_8$]$^{12+}$ (%)	Py* (%)	**Int** (%)	$\langle a\rangle$	$\langle b\rangle$	$\langle c\rangle$	$\langle n\rangle$	$\langle k\rangle$
0	100	100	0	0	0	–	–	–	–	–
5	31.8	15.8	11.9	41.8	72.3	0.181	0.309	0.338	1.24	0.584
10	17.6	10.9	15.4	56.7	73.7	0.215	0.316	0.330	1.68	0.682
15	11.1	9.4	19.6	66.6	71.0	0.222	0.304	0.286	1.98	0.731
20	8.6	8.4	23.1	71.2	68.5	0.220	0.293	0.259	2.11	0.748
25	7.8	7.9	25.9	75.7	66.1	0.213	0.283	0.211	2.26	0.751
30	6.6	7.5	28.5	78.1	64.0	0.209	0.274	0.197	2.32	0.761
35	6.2	7.1	31.2	82.1	61.7	0.201	0.264	0.151	2.47	0.761
40	5.4	6.8	33.3	83.1	59.9	0.197	0.257	0.148	2.49	0.768
45	5.2	6.5	33.9	83.1	59.6	0.196	0.255	0.150	2.48	0.766
50	4.6	6.2	36.6	85.6	57.1	0.189	0.245	0.126	2.57	0.772
55	4.4	6.1	38.1	86.3	55.8	0.185	0.239	0.119	2.59	0.773
60	4.4	5.7	39.9	86.3	54.4	0.179	0.233	0.120	2.56	0.769
75	4.3	5.5	40.7	87.2	53.7	0.176	0.230	0.110	2.59	0.767
90	4.3	5.3	41.3	88.0	53.4	0.175	0.229	0.099	2.63	0.765
105	4.2	5.0	42.4	88.8	52.6	0.171	0.225	0.090	2.65	0.762
120	4.0	4.7	42.6	89.5	52.8	0.172	0.226	0.083	2.67	0.760
180	4.0	3.9	46.8	90.3	49.3	0.158	0.211	0.074	2.65	0.749
240	3.9	3.8	49.9	90.8	46.3	0.148	0.198	0.067	2.65	0.748
300	3.7	3.7	51.5	91.0	44.7	0.144	0.192	0.067	2.65	0.750
360	3.6	3.7	54.2	91.6	42.2	0.136	0.181	0.062	2.66	0.750
420	3.6	3.6	55.1	91.6	41.3	0.132	0.177	0.062	2.65	0.750
480	3.5	3.5	55.5	92.3	41.0	0.132	0.176	0.055	2.69	0.751
540	3.4	3.5	55.9	93.1	40.7	0.131	0.174	0.045	2.74	0.751
720	3.4	3.4	57.1	93.9	39.5	0.127	0.169	0.035	2.79	0.750
1440	3.4	3.3	60.7	93.8	36.0	0.115	0.154	0.037	2.76	0.749

Table S4. Time variation of **1***, $PdPy*_4(OTf)_2$, Py*, Pd_6**1***$_8(OTf)_{12}$, and **Int** and $\langle a \rangle$–$\langle c \rangle$ of the average composition of **Int**, $Pd_{\langle a \rangle}$**1***$_{\langle b \rangle}$Py*$_{\langle c \rangle}$, and the ($\langle n \rangle$, $\langle k \rangle$) values for the self-assembly of the Pd_6**1***$_8(OTf)_{12}$ capsule from **1*** and $PdPy*_4(OTf)_2$ in CD_3NO_2/CD_2Cl_2 (v/v = 4/1) at 298 K ([**1***]$_0$ = 2.2 mM) (run 3).

Time (min)	$[PdPy*_4]^{2+}$ (%)	**1*** (%)	$[Pd_6$**1***$_8]^{12+}$ (%)	Py* (%)	**Int** (%)	$\langle a \rangle$	$\langle b \rangle$	$\langle c \rangle$	$\langle n \rangle$	$\langle k \rangle$
0	100	100	0	0	0	–	–	–	–	–
5	32.5	16.0	12.1	46.1	71.9	0.179	0.310	0.277	1.42	0.577
10	20.5	14.4	14.4	61.2	71.1	0.210	0.307	0.237	1.97	0.686
15	10.2	10.4	22.6	69.8	66.9	0.218	0.289	0.260	2.11	0.753
20	8.9	10.0	27.4	77.6	62.7	0.206	0.271	0.176	2.40	0.763
25	7.7	9.3	29.1	82.6	61.6	0.205	0.266	0.126	2.61	0.770
30	7.0	8.0	30.2	84.9	61.8	0.203	0.267	0.104	2.66	0.762
35	5.8	7.8	31.4	85.8	60.8	0.203	0.262	0.110	2.68	0.775
40	5.0	6.6	32.5	86.3	60.9	0.202	0.263	0.113	2.65	0.771
45	4.8	6.1	33.4	86.5	60.5	0.200	0.261	0.112	2.64	0.766
50	4.7	5.8	34.8	87.1	59.4	0.196	0.256	0.107	2.64	0.764
55	4.5	5.5	34.4	87.1	60.1	0.198	0.259	0.109	2.63	0.762
60	4.3	5.2	35.4	88.3	59.3	0.195	0.256	0.095	2.67	0.762
75	4.1	5.1	37.9	88.3	57.0	0.188	0.246	0.097	2.65	0.763
90	4.0	5.0	40.4	88.4	54.6	0.180	0.236	0.099	2.63	0.764
105	3.8	4.9	42.2	88.5	52.9	0.175	0.228	0.100	2.63	0.765
120	3.6	4.8	44.7	88.5	50.5	0.167	0.218	0.102	2.60	0.768
180	3.3	4.5	46.4	89.2	49.1	0.163	0.212	0.098	2.61	0.768
240	3.3	4.1	47.9	90.4	48.0	0.158	0.207	0.082	2.66	0.763
300	3.3	3.8	49.7	90.4	46.5	0.152	0.201	0.082	2.63	0.758
360	3.3	3.5	50.6	90.9	45.9	0.149	0.198	0.075	2.63	0.753
420	3.3	3.1	51.0	91.1	45.9	0.148	0.198	0.073	2.62	0.747
480	3.3	3.1	51.9	91.2	45.0	0.145	0.194	0.072	2.62	0.747
540	3.3	3.1	53.5	91.6	43.4	0.140	0.187	0.067	2.63	0.747
720	3.3	3.1	56.2	91.6	40.7	0.131	0.176	0.066	2.61	0.747
1440	3.3	3.1	57.8	91.7	39.1	0.126	0.169	0.065	2.60	0.747

Table S5. Time variation of racemic **1**, $PdPy*_4(OTf)_2$, Py*, $Pd_6\mathbf{1}_8(OTf)_{12}$, and **Int** and the ($\langle n \rangle$, $\langle k \rangle$) values for the self-assembly of the $Pd_6\mathbf{1}_8(OTf)_{12}$ capsule from racemic **1** and $PdPy*_4(OTf)_2$ in CD_3NO_2/CD_2Cl_2 (v/v = 4/1) at 298 K ($[\mathbf{1}]_0$ = 2.2 mM).

Time (min)	$[PdPy*_4]^{2+}$ (%)	**1** (%)	$[Pd_6\mathbf{1}_8]^{12+}$ (%)	Py* (%)	**Int** (%)	$[PdPy*_4]^{2+}$ SE	**1** SE	$[Pd_6\mathbf{1}_8]^{12+}$ SE	Py* SE	**Int** SE
0	100	100	0	0	0	0	0	0	0	0
5	28.5	16.8	4.9	44.8	78.3	1.98	2.03	0.066	2.63	2.08
10	16.9	12.6	5.7	54.3	81.8	1.02	1.11	0.13	1.70	1.24
15	12.0	10.9	6.8	65.7	82.3	0.234	0.700	0.17	1.17	0.866
20	9.2	10.0	7.4	70.9	82.6	0.228	0.544	0.382	0.877	0.917
25	7.7	9.4	7.6	72.9	83.0	0.097	0.352	0.376	1.17	0.713
30	6.7	8.9	7.8	76.0	83.3	0.243	0.320	0.402	0.926	0.717
35	6.2	8.7	8.0	78.2	83.4	0.132	0.362	0.437	0.766	0.799
40	5.7	8.4	8.2	79.5	83.5	0.426	0.331	0.496	0.935	0.827
45	5.2	8.0	8.5	80.2	83.5	0.136	0.323	0.502	0.955	0.819
50	5.0	7.7	9.4	81.1	82.9	0.220	0.301	0.379	0.932	0.440
55	4.8	7.6	10.4	81.9	82.0	0.235	0.264	0.747	0.800	0.666
60	4.7	7.5	11.5	82.6	81.0	0.304	0.214	1.10	1.07	0.991
75	4.6	7.2	13.2	83.5	79.7	0.283	0.082	1.54	1.12	1.46
90	4.5	6.7	14.9	84.4	78.4	0.275	0.167	1.64	1.20	1.48
105	4.4	6.5	17.1	85.1	76.4	0.298	0.219	1.51	1.12	1.36
120	4.2	6.1	20.1	85.9	73.8	0.306	0.213	0.752	1.25	0.784
180	3.9	5.7	21.1	86.1	73.2	0.302	0.106	0.771	1.18	0.729
240	3.9	5.5	21.5	86.6	73.0	0.307	0.186	0.512	1.01	0.333
300	4.0	5.2	22.0	86.8	72.8	0.367	0.160	0.490	1.06	0.337
360	3.7	5.0	22.5	87.0	72.5	0.396	0.165	0.505	1.09	0.348
420	3.7	5.0	22.6	87.3	72.4	0.411	0.196	0.522	1.05	0.327
480	3.9	4.9	23.3	87.6	71.8	0.529	0.181	0.642	1.01	0.498
540	3.9	4.9	23.8	88.1	71.3	0.569	0.178	0.570	1.09	0.438
720	3.7	4.9	24.1	88.5	71.0	0.419	0.229	0.788	1.15	0.632
1440	3.6	4.4	25.9	88.9	69.7	0.472	0.412	1.05	0.891	1.25

*SE = Standard error.

Time (min)	$\langle n \rangle$	$\langle k \rangle$	$\langle n \rangle$ SE	$\langle k \rangle$ SE
5	1.53	0.638	0.071	0.007
10	1.79	0.710	0.049	0.005
15	2.15	0.740	0.032	0.004
20	2.30	0.758	0.027	0.005
25	2.36	0.766	0.036	0.003
30	2.46	0.769	0.028	0.005
35	2.53	0.772	0.020	0.004
40	2.57	0.774	0.026	0.004
45	2.57	0.775	0.028	0.003
50	2.60	0.775	0.025	0.003
55	2.61	0.776	0.019	0.004
60	2.63	0.775	0.030	0.004
75	2.65	0.774	0.037	0.003
90	2.66	0.772	0.043	0.003
105	2.67	0.770	0.040	0.004
120	2.67	0.769	0.048	0.005
180	2.66	0.769	0.044	0.004
240	2.68	0.766	0.038	0.004
300	2.67	0.763	0.041	0.004
360	2.67	0.764	0.043	0.005
420	2.68	0.763	0.039	0.005
480	2.69	0.761	0.040	0.005
540	2.71	0.760	0.043	0.005
720	2.72	0.763	0.048	0.004
1440	2.71	0.758	0.050	0.001

Table S6. Time variation of racemic **1**, $PdPy*_4(OTf)_2$, Py*, $Pd_6\mathbf{1}_8(OTf)_{12}$, and **Int** and $\langle a\rangle$–$\langle c\rangle$ of the average composition of **Int**, $Pd_{\langle a\rangle}\mathbf{1}_{\langle b\rangle}Py*_{\langle c\rangle}$, and the ($\langle n\rangle$, $\langle k\rangle$) values for the self-assembly of the $Pd_6\mathbf{1*}_8(OTf)_{12}$ capsule from racemic **1** and $PdPy*_4(OTf)_2$ in CD_3NO_2/CD_2Cl_2 (v/v = 4/1) at 298 K ($[\mathbf{1}]_0$ = 2.2 mM) (run 1).

Time (min)	$[PdPy*_4]^{2+}$ (%)	**1** (%)	$[Pd_6\mathbf{1}_8]^{12+}$ (%)	Py* (%)	**Int** (%)	$\langle a\rangle$	$\langle b\rangle$	$\langle c\rangle$	$\langle n\rangle$	$\langle k\rangle$
0	100	100	0	0	0	–	–	–	–	–
5	32.4	20.8	5.0	39.9	74.2	0.200	0.315	0.354	1.41	0.633
10	18.9	14.6	5.9	53.1	79.5	0.240	0.338	0.356	1.78	0.709
15	12.3	12.0	7.2	63.4	80.8	0.257	0.344	0.310	2.09	0.747
20	9.5	10.8	8.1	69.1	81.1	0.263	0.345	0.272	2.26	0.762
25	7.5	9.9	8.2	70.9	81.9	0.269	0.348	0.276	2.29	0.771
30	6.3	9.4	8.5	74.1	82.2	0.272	0.349	0.249	2.40	0.778
35	6.0	9.3	8.8	77.0	81.9	0.272	0.348	0.217	2.50	0.781
40	5.4	8.9	9.0	77.9	82.1	0.273	0.349	0.212	2.52	0.782
45	5.0	8.5	9.4	78.4	82.1	0.273	0.349	0.211	2.52	0.781
50	4.7	8.2	9.8	79.6	82.0	0.273	0.349	0.200	2.55	0.782
55	4.4	8.0	10.4	80.9	81.6	0.272	0.347	0.187	2.59	0.783
60	4.3	7.8	11.6	80.9	80.6	0.268	0.342	0.189	2.58	0.783
75	4.1	7.2	13.0	81.6	79.7	0.264	0.339	0.183	2.58	0.779
90	4.0	6.7	15.8	82.4	77.4	0.256	0.329	0.174	2.58	0.777
105	3.8	6.6	18.4	83.1	75.0	0.248	0.319	0.167	2.59	0.778
120	3.6	6.3	21.5	83.6	72.3	0.239	0.307	0.164	2.58	0.778
180	3.4	5.8	21.5	84.0	72.7	0.240	0.309	0.160	2.58	0.775
240	3.3	5.5	21.5	84.8	72.9	0.240	0.310	0.152	2.60	0.773
300	3.3	5.3	22.0	84.8	72.7	0.238	0.309	0.152	2.59	0.771
360	3.0	5.0	22.3	84.9	72.7	0.238	0.309	0.155	2.58	0.771
420	2.9	5.1	22.3	85.3	72.5	0.238	0.308	0.150	2.60	0.773
480	2.9	4.9	22.7	85.6	72.4	0.237	0.308	0.146	2.61	0.770
540	2.9	4.9	23.2	86.0	72.0	0.236	0.306	0.141	2.62	0.771
720	2.9	4.8	23.3	86.2	71.9	0.235	0.305	0.139	2.63	0.770
1440	2.7	3.6	24.6	87.1	71.8	0.232	0.305	0.130	2.61	0.759

Table S7. Time variation of racemic **1**, $PdPy^*_4(OTf)_2$, Py*, $Pd_6\mathbf{1}_8(OTf)_{12}$, and **Int** and $\langle a \rangle$–$\langle c \rangle$ of the average composition of **Int**, $Pd_{\langle a \rangle}\mathbf{1}_{\langle b \rangle}Py^*_{\langle c \rangle}$, and the ($\langle n \rangle$, $\langle k \rangle$) values for the self-assembly of the $Pd_6\mathbf{1}^*_8(OTf)_{12}$ capsule from racemic **1** and $PdPy^*_4(OTf)_2$ in CD_3NO_2/CD_2Cl_2 (v/v = 4/1) at 298 K ([**1**]$_0$ = 2.2 mM) (run 2).

Time (min)	$[PdPy^*_4]^{2+}$ (%)	**1** (%)	$[Pd_6\mathbf{1}_8]^{12+}$ (%)	Py* (%)	**Int** (%)	$\langle a \rangle$	$\langle b \rangle$	$\langle c \rangle$	$\langle n \rangle$	$\langle k \rangle$
0	100	100	0	0	0	–	–	–	–	–
5	25.8	15.5	4.9	48.9	79.6	0.221	0.338	0.322	1.66	0.652
10	15.6	12.3	5.7	52.2	82.1	0.251	0.349	0.410	1.70	0.720
15	12.1	11.1	6.8	66.9	82.1	0.259	0.349	0.268	2.20	0.741
20	8.7	10.2	7.3	72.0	82.5	0.268	0.351	0.246	2.35	0.763
25	7.8	9.6	7.5	73.0	82.9	0.270	0.352	0.244	2.37	0.766
30	6.8	9.0	7.7	76.7	83.2	0.272	0.354	0.211	2.48	0.770
35	6.4	8.6	8.0	77.8	83.5	0.273	0.355	0.201	2.51	0.769
40	6.6	8.5	8.2	79.5	83.4	0.272	0.354	0.178	2.57	0.767
45	5.5	8.1	8.4	80.4	83.5	0.275	0.355	0.180	2.59	0.774
50	5.4	7.9	8.6	81.0	83.5	0.274	0.355	0.173	2.60	0.772
55	5.2	7.5	9.1	81.3	83.3	0.273	0.354	0.173	2.60	0.771
60	5.3	7.5	9.6	82.3	82.9	0.271	0.352	0.159	2.63	0.770
75	5.1	7.3	10.6	83.4	82.2	0.269	0.349	0.147	2.66	0.770
90	4.9	7.0	11.7	84.2	81.3	0.266	0.345	0.139	2.68	0.769
105	4.8	6.7	14.1	85.1	79.2	0.259	0.336	0.129	2.69	0.769
120	4.4	6.3	18.9	86.1	74.9	0.244	0.318	0.120	2.70	0.768
180	3.7	5.7	19.6	86.2	74.7	0.244	0.317	0.128	2.68	0.770
240	4.1	5.8	20.6	86.9	73.6	0.240	0.313	0.115	2.70	0.767
300	4.4	5.5	21.1	87.0	73.4	0.237	0.312	0.109	2.69	0.761
360	3.9	5.3	21.7	87.4	73.0	0.237	0.310	0.110	2.70	0.764
420	4.2	5.2	21.9	87.9	72.9	0.235	0.310	0.101	2.72	0.760
480	4.7	5.2	22.7	88.2	72.1	0.231	0.306	0.090	2.73	0.755
540	4.9	5.2	23.3	88.6	71.5	0.229	0.304	0.084	2.74	0.754
720	4.3	5.3	23.3	89.3	71.4	0.231	0.303	0.081	2.77	0.761
1440	4.3	5.0	25.2	89.6	69.8	0.225	0.297	0.077	2.77	0.757

Table S8. Time variation of racemic **1**, $PdPy*_4(OTf)_2$, Py*, $Pd_6\mathbf{1}_8(OTf)_{12}$, and **Int** and $\langle a \rangle$–$\langle c \rangle$ of the average composition of **Int**, $Pd_{\langle a \rangle}\mathbf{1}_{\langle b \rangle}Py*_{\langle c \rangle}$, and the ($\langle n \rangle$, $\langle k \rangle$) values for the self-assembly of the $Pd_6\mathbf{1}*_8(OTf)_{12}$ capsule from racemic **1** and $PdPy*_4(OTf)_2$ in CD_3NO_2/CD_2Cl_2 (v/v = 4/1) at 298 K ($[\mathbf{1}]_0$ = 2.2 mM) (run 3).

Time (min)	$[PdPy*_4]^{2+}$ (%)	**1** (%)	$[Pd_6\mathbf{1}_8]^{12+}$ (%)	Py* (%)	**Int** (%)	$\langle a \rangle$	$\langle b \rangle$	$\langle c \rangle$	$\langle n \rangle$	$\langle k \rangle$
0	100	100	0	0	0	–	–	–	–	–
5	27.4	14.2	4.8	45.5	81.1	0.221	0.351	0.353	1.51	0.628
10	16.2	10.8	5.4	57.7	83.7	0.255	0.363	0.339	1.87	0.701
15	11.5	9.6	6.6	66.9	83.8	0.266	0.363	0.281	2.16	0.733
20	9.2	9.0	6.8	71.4	84.3	0.273	0.365	0.252	2.30	0.748
25	7.6	8.7	6.9	74.9	84.4	0.278	0.366	0.228	2.42	0.760
30	7.1	8.3	7.1	77.1	84.6	0.279	0.367	0.205	2.48	0.760
35	6.2	8.1	7.3	79.6	84.7	0.281	0.367	0.184	2.56	0.766
40	5.2	7.8	7.3	81.2	84.9	0.284	0.368	0.177	2.61	0.773
45	5.1	7.4	7.6	81.6	85.0	0.284	0.368	0.173	2.61	0.770
50	4.9	7.2	9.7	82.8	83.2	0.278	0.360	0.160	2.64	0.771
55	4.7	7.1	11.7	83.5	81.2	0.272	0.352	0.154	2.65	0.773
60	4.6	7.1	13.4	84.6	79.6	0.267	0.345	0.140	2.69	0.773
75	4.6	7.0	15.9	85.4	77.1	0.258	0.334	0.129	2.71	0.773
90	4.6	6.4	17.2	86.5	76.4	0.254	0.331	0.116	2.72	0.768
105	4.6	6.0	18.8	87.0	75.2	0.249	0.326	0.110	2.72	0.765
120	4.5	5.6	20.1	87.9	74.3	0.245	0.322	0.098	2.74	0.761
180	4.4	5.5	22.2	88.1	72.3	0.239	0.313	0.097	2.74	0.761
240	4.3	5.1	22.4	88.2	72.5	0.238	0.314	0.097	2.73	0.758
300	4.3	4.9	22.8	88.5	72.3	0.237	0.313	0.094	2.73	0.757
360	4.3	4.8	23.4	88.6	71.8	0.235	0.311	0.092	2.72	0.755
420	4.1	4.6	23.6	88.8	71.8	0.235	0.311	0.093	2.72	0.755
480	4.0	4.6	24.6	88.9	70.8	0.232	0.307	0.092	2.73	0.756
540	4.0	4.6	24.9	89.8	70.5	0.231	0.305	0.082	2.76	0.757
720	3.9	4.5	25.7	89.9	69.8	0.229	0.302	0.080	2.76	0.757
1440	3.7	4.5	28.0	90.0	67.5	0.222	0.292	0.082	2.75	0.759

ESI-TOF mass study of the self-assembly of the $Pd_6\mathbf{1}_8(OTf)_{12}$ capsule

Time-dependent ESI-TOF mass spectra were measured to investigate the intermediates. The self-assembly of $Pd_6\mathbf{1}_8(OTf)_{12}$ from **1** (**1*** or racemic **1**) (1.2 μmol, $[\mathbf{1}]_0$ = 2.2 mM) and PdPy*$_4$(OTf)$_2$ (0.9 μmol) in CH_3NO_2/CH_2Cl_2 (*ca.* 550 μL) at 298 K was carried out in the same way as monitoring the self-assembly of the $Pd_6\mathbf{1}_8(OTf)_{12}$ capsule (see: section "Procedure for Monitoring the Self-Assembly Process of the $Pd_6\mathbf{1}_8(OTf)_{12}$ capsule"). At each time, 50 μL of the reaction mixture was taken, diluted with CH_3NO_2 (500 μL), filtered through a membrane filter (pore size: 0.20 μm), and injected to the mass spectrometer with 5 μL/min flow rate to obtain ESI-TOF mass spectra, which are shown in Figure S2 for the self-assembly from **1*** and in Figure S3 for the self-assembly from racemic **1**. The time evolution of the species is summarized in Table 1 for the self-assembly from **1*** and in Table S9 for the self-assembly from racemic **1**.

Table S9. The time evolution of the species for the self-assembly of the $Pd_6\mathbf{1}_8$ capsule from racemic **1** and PdPy*$_4$(OTf)$_2$ in CD_3NO_2 and CD_2Cl_2 (v/v = 4/1) at 298 K.

5 min	10 min	30 min	60 min	120 min	180 min	360 min
(1,1,0)[a]	(1,1,0)	(1,1,0)	(1,1,0)	(1,1,0)	(1,1,0)	(1,1,0)
(1,1,1)	(1,1,1)	(1,1,1)	(1,1,1)	(1,1,1)	(1,1,1)	(1,1,1)
(1,1,2)	(1,1,2)	(1,1,2)	(1,1,2)	(1,1,2)	(1,1,2)	(1,1,2)
(1,2,0)	(1,2,0)	(1,2,0)	(1,2,0)	(1,2,0)	(1,2,0)	(1,2,0)
(2,2,0)	(2,2,0)	(2,2,0)	(2,2,0)	(2,2,0)	(2,2,0)	(2,2,0)
		(2,3,0)	(2,3,0)	(2,3,0)	(2,3,0)	(2,3,0)
	(3,8,3)	(3,8,3)	(3,8,3)	(3,8,3)	(3,8,3)	(3,8,3)
	(6,8,0)	(6,8,0)	(6,8,0)	(6,8,0)	(6,8,0)	(6,8,0)

[a]Underlines indicate the species whose Pd(II) ion(s) is/are coordinately unsaturated.

(a)

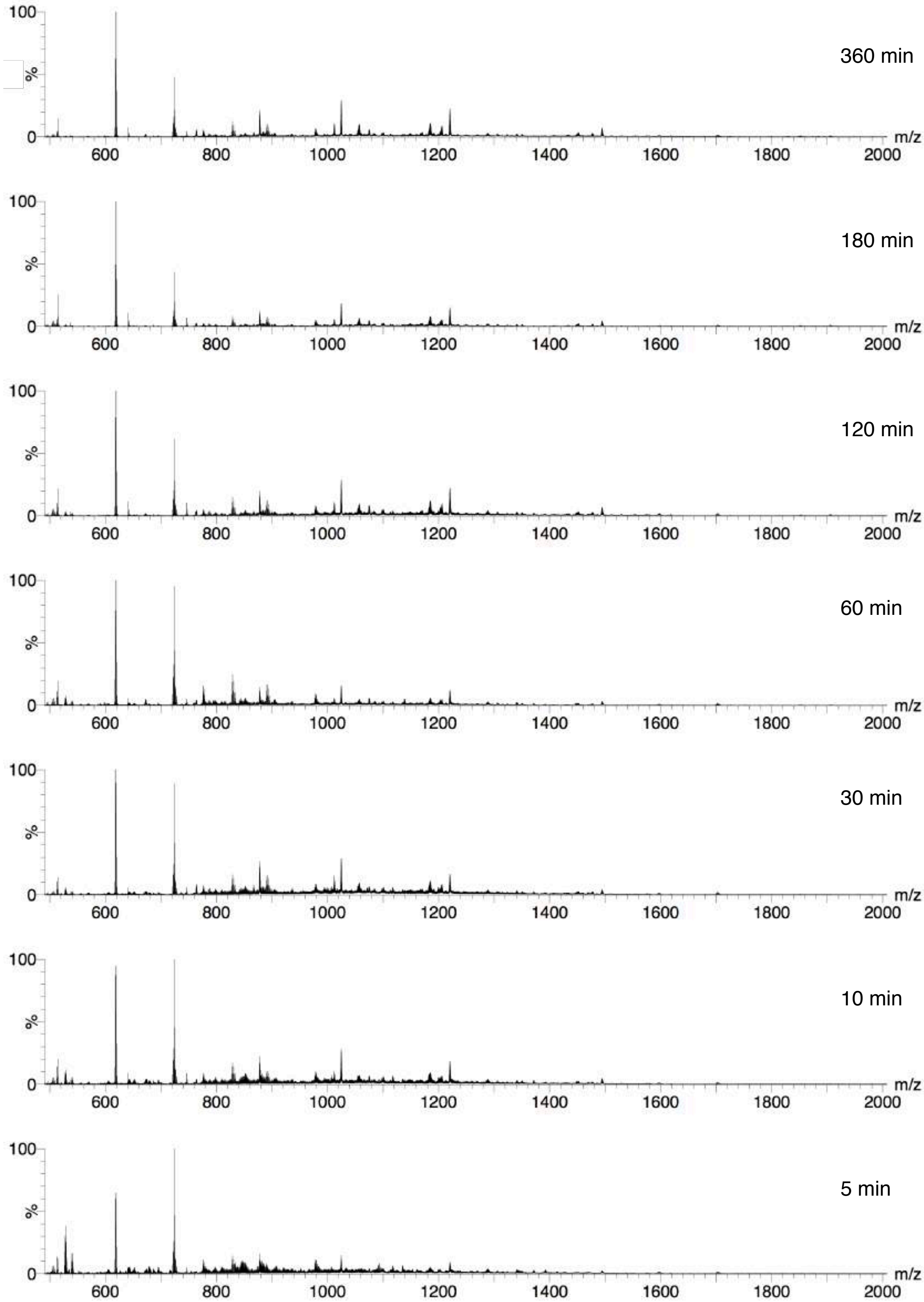

Figure S2. (a) Time-dependent ESI-TOF mass spectra of the reaction mixture for the self-assembly of the $Pd_6\mathbf{1}*_8(OTf)_{12}$ capsule from **1*** and $PdPy*_4(OTf)_2$. (b) Magnified ESI-TOF mass spectra of (a) (*m/z* 500–1300). (c) Magnified ESI-TOF mass spectra of (a) (*m/z* 1300–2000). (d)–(q) Magnified ESI-TOF mass spectra for the region of $[Pd\mathbf{1}*Py*_2]^{2+}$ (d); $[\mathbf{1}*\cdot H_2 - COPy]^{+}$ and $[\mathbf{1}*\cdot H - COPy]^{+}$ (e); $[Pd_2\mathbf{1}_2Py*_2(OTf)]^{3+}$ (f); $[\mathbf{1}*\cdot H]^{+}$ (g); $[Pd\mathbf{1}_2]^{2+}$ (h); $[Pd_6\mathbf{1}_8(OTf)_4]^{8+}$ and $[Pd_6\mathbf{1}*_8(OTf)_3(NO_3)]^{8+}$ (i); $[Pd\mathbf{1}*(OTf)]^{+}$ and $[Pd_2\mathbf{1}*_2(OTf)_2]^{2+}$ (j); $[Pd_6\mathbf{1}*_8(OTf)_5]^{7+}$ and $[Pd_6\mathbf{1}*_8(OTf)_4(NO_3)]^{7+}$ (k); $[Pd_3\mathbf{1}*_8Py*_3]^{6+}$ (l); $[Pd_6\mathbf{1}*_8(OTf)_6]^{6+}$ and $[Pd_6\mathbf{1}*_8(OTf)_5(NO_3)]^{6+}$ (m); $[Pd_2\mathbf{1}*_3(OTf)_2]^{2+}$ (n); $[Pd_6\mathbf{1}*_8(OTf)_7]^{5+}$ and $[Pd_6\mathbf{1}*_8(OTf)_6(NO_3)]^{5+}$ (o); $[Pd\mathbf{1}*_2(OTf)]^{+}$ (p); $[Pd_6\mathbf{1}*_8(OTf)_8]^{4+}$ (q).

(b)

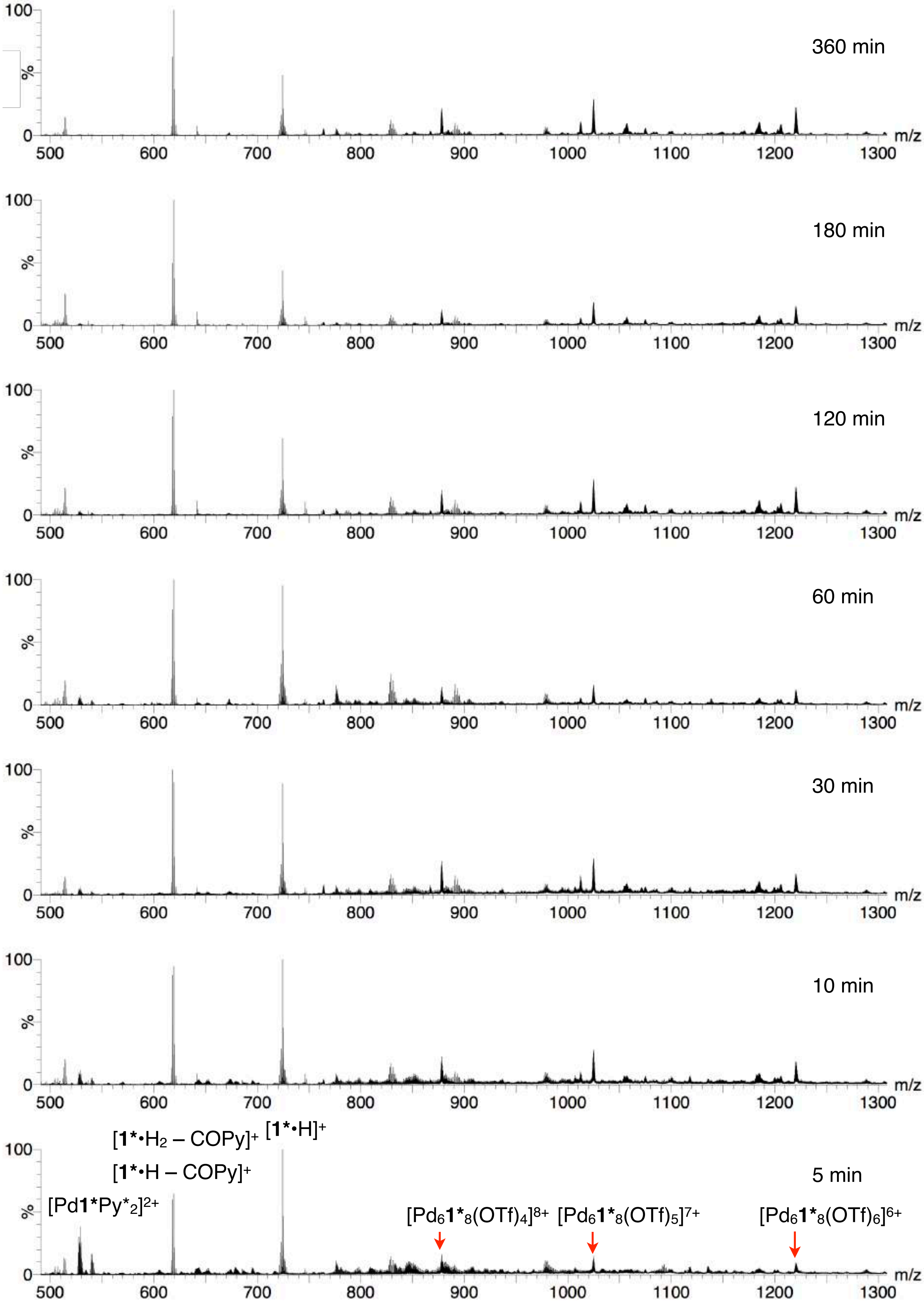

360 min
180 min
120 min
60 min
30 min
10 min
5 min
100
%
0
m/z
500
600
700
800
900
1000
1100
1200
1300
[1*•H2 – COPy]+
[1*•H]+
[1*•H – COPy]+
[Pd1*Py*2]2+
[Pd61*8(OTf)4]8+
[Pd61*8(OTf)5]7+
[Pd61*8(OTf)6]6+

(c)

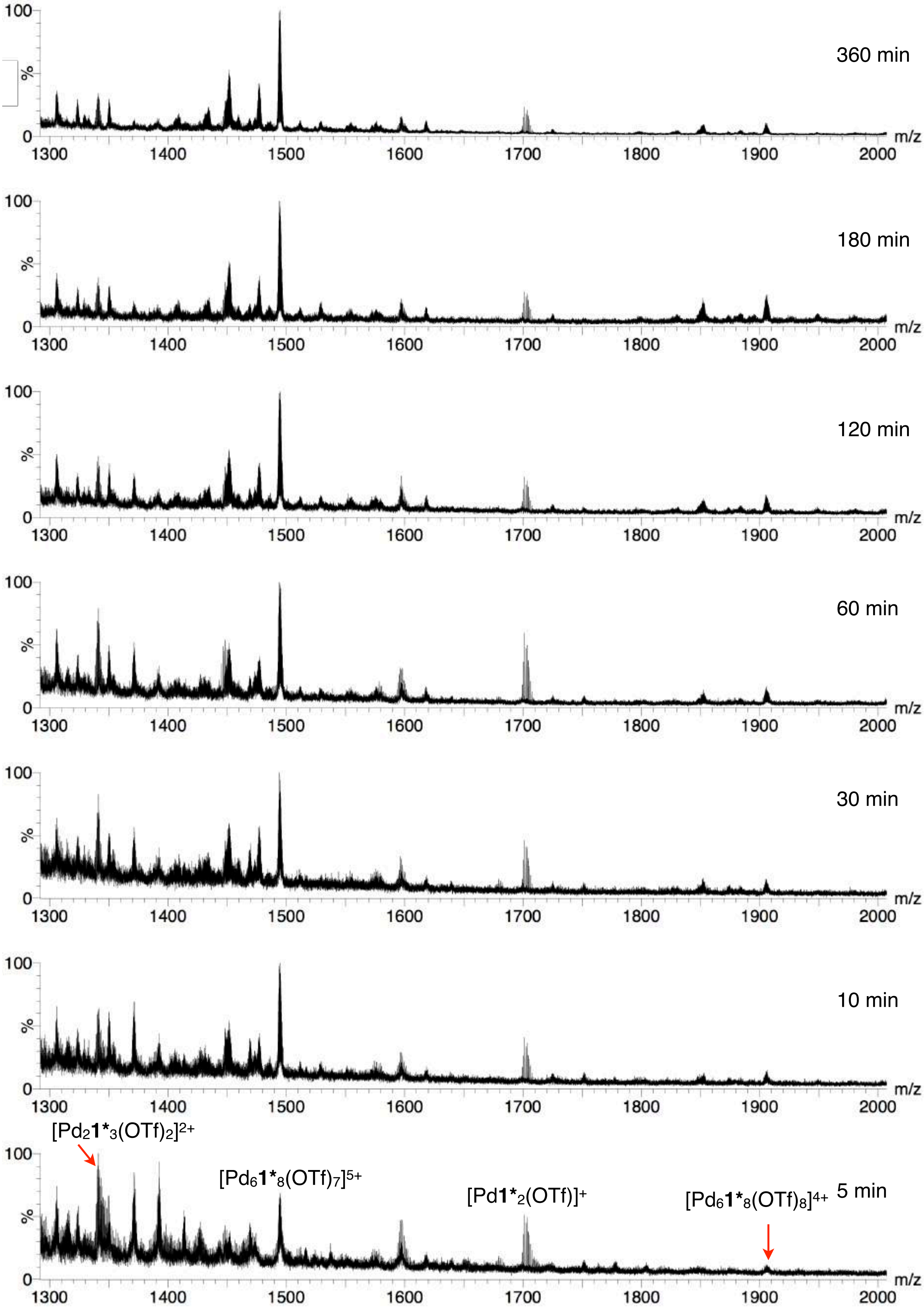
360 min
180 min
120 min
60 min
30 min
10 min
5 min
[Pd$_2$**1***$_3$(OTf)$_2$]$^{2+}$
[Pd$_6$**1***$_8$(OTf)$_7$]$^{5+}$
[Pd**1***$_2$(OTf)]$^+$
[Pd$_6$**1***$_8$(OTf)$_8$]$^{4+}$
%
m/z
100
0
1300
1400
1500
1600
1700
1800
1900
2000

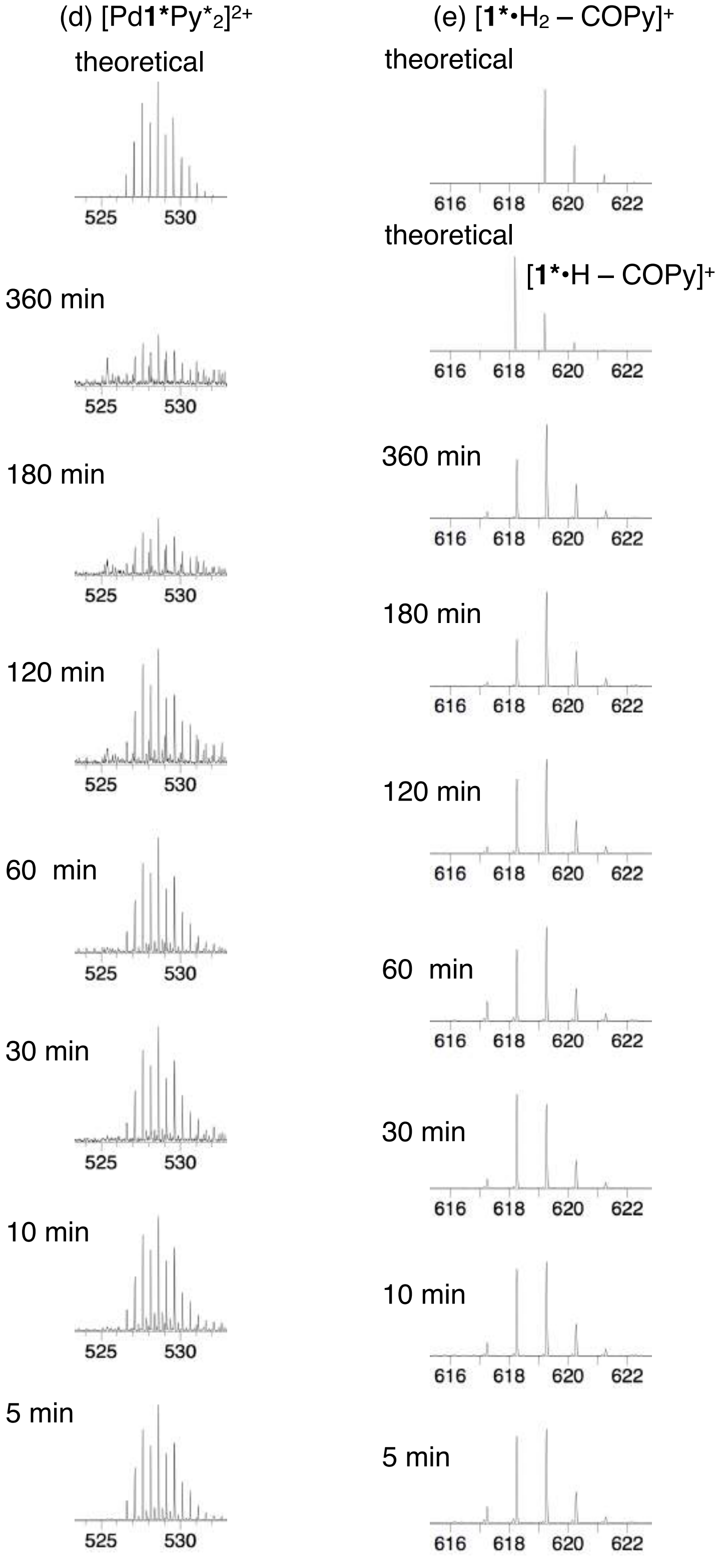
(d) [Pd1*Py*2]2+
theoretical
525
530
360 min
180 min
120 min
60 min
30 min
10 min
5 min
(e) [1*•H2 – COPy]+
theoretical
616
618
620
622
theoretical
[1*•H – COPy]+
360 min
180 min
120 min
60 min
30 min
10 min
5 min
(f) [Pd21*2Py*2(OTf)]3+
theoretical
680
360 min
180 min
120 min
60 min
30 min
10 min
5 min

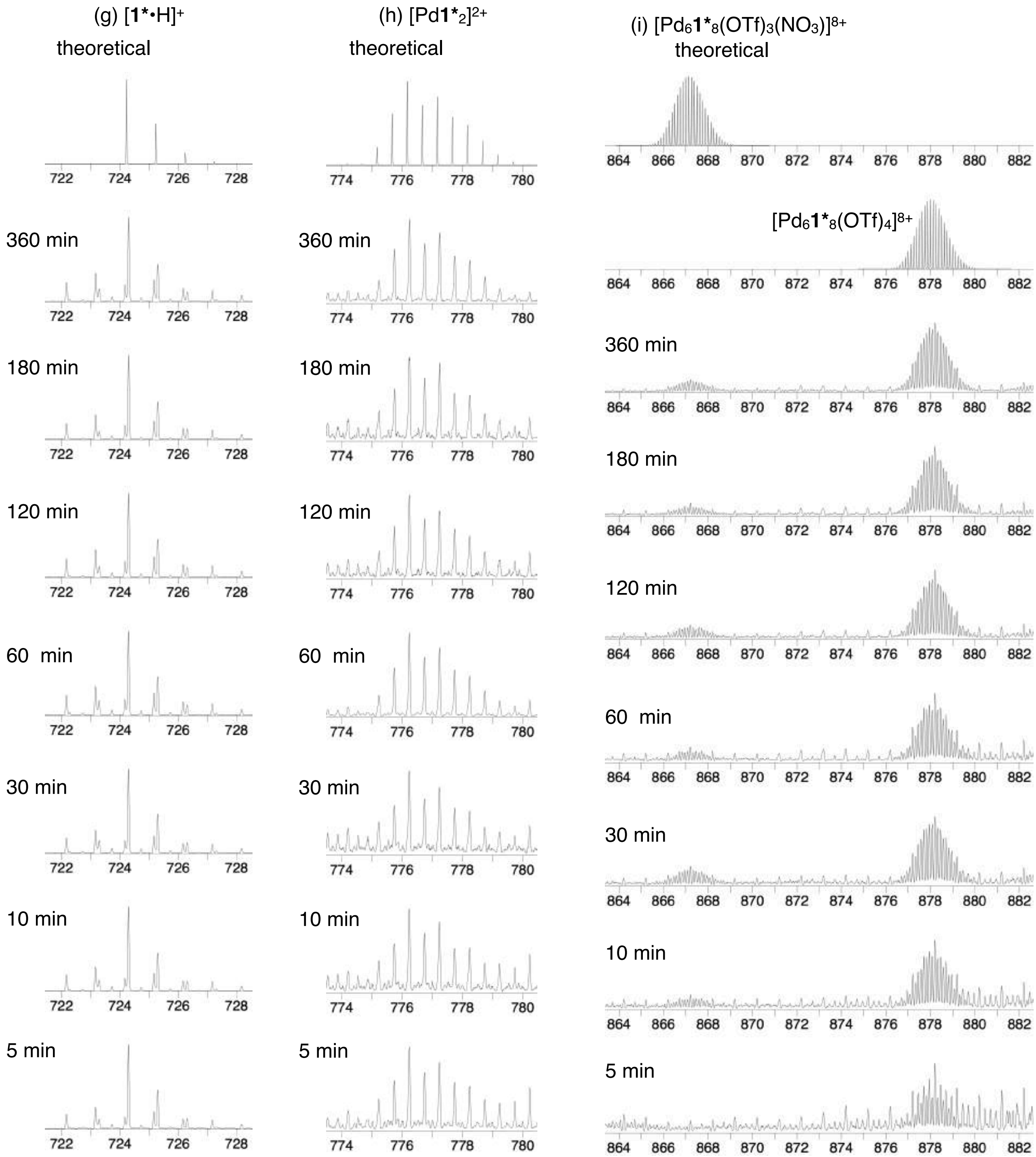

(g) [1*•H]+
theoretical
360 min
180 min
120 min
60 min
30 min
10 min
5 min
722 724 726 728
(h) [Pd1*2]2+
theoretical
360 min
180 min
120 min
60 min
30 min
10 min
5 min
774 776 778 780
(i) [Pd61*8(OTf)3(NO3)]8+
theoretical
[Pd61*8(OTf)4]8+
360 min
180 min
120 min
60 min
30 min
10 min
5 min
864 866 868 870 872 874 876 878 880 882

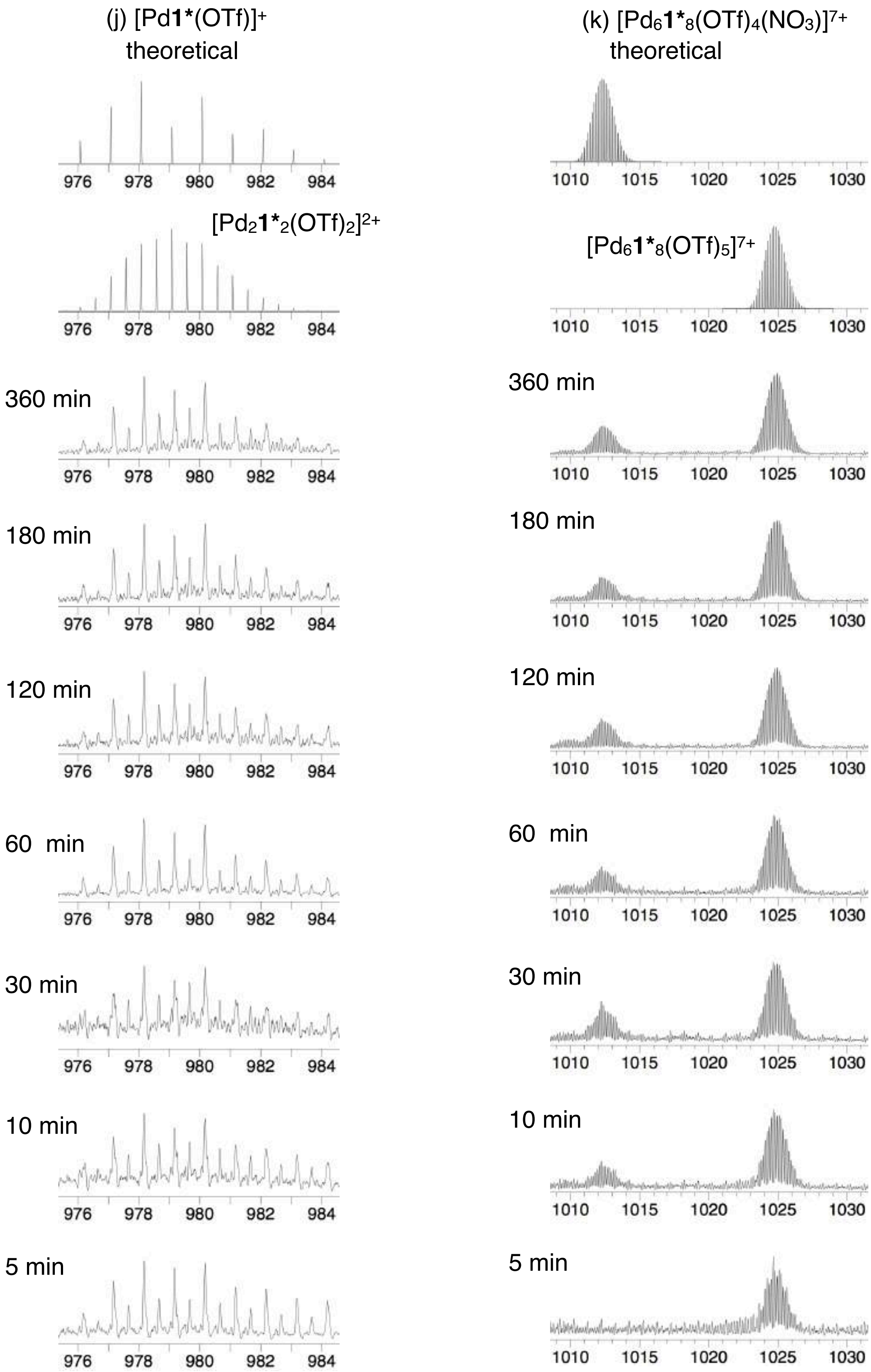
(j) [Pd1*(OTf)]+
theoretical
[Pd21*2(OTf)2]2+
360 min
180 min
120 min
60 min
30 min
10 min
5 min
976
978
980
982
984
(k) [Pd61*8(OTf)4(NO3)]7+
theoretical
[Pd61*8(OTf)5]7+
1010
1015
1020
1025
1030

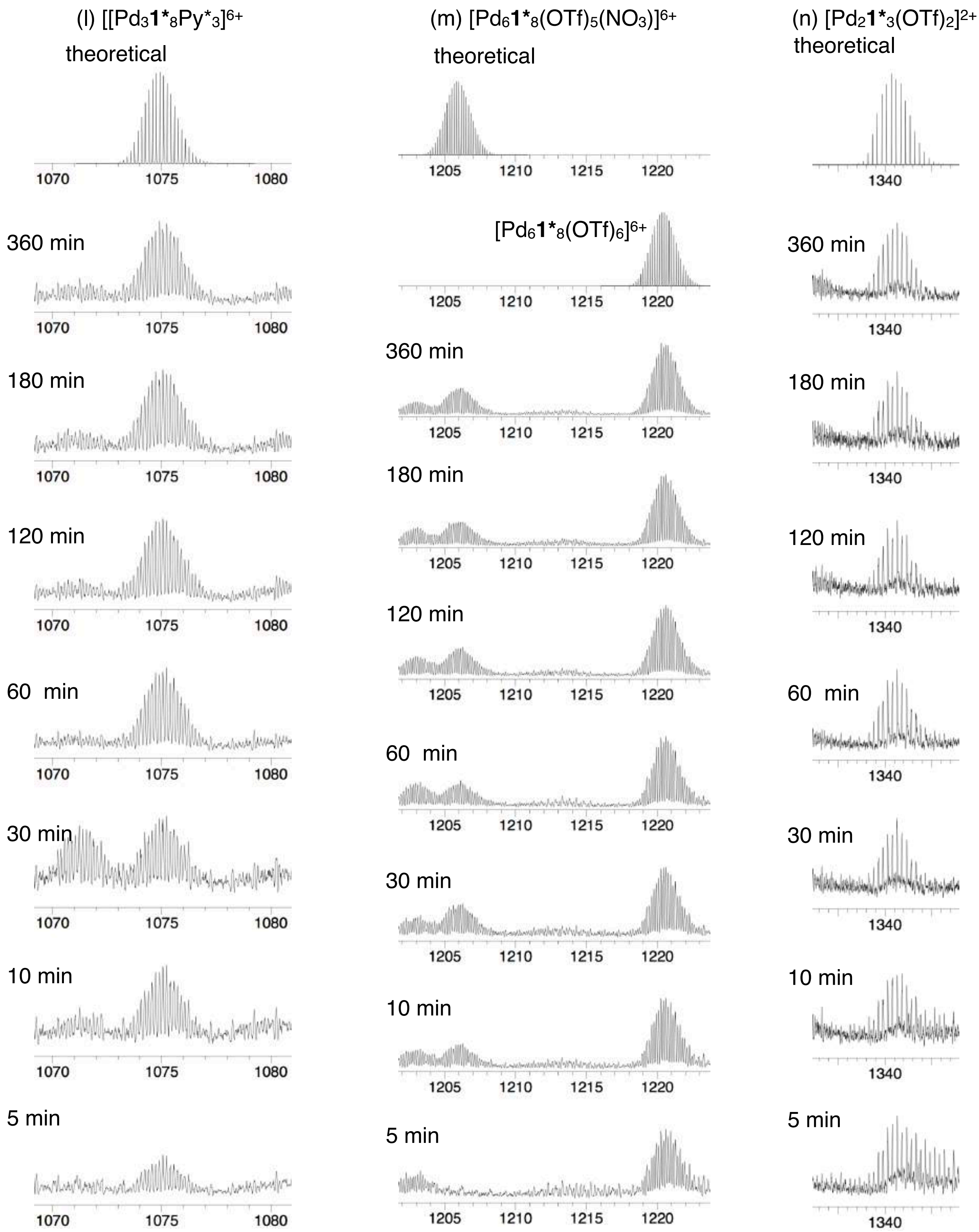
(l) [[Pd_3**1***$_8$Py*$_3$]$^{6+}$
theoretical
360 min
180 min
120 min
60 min
30 min
10 min
5 min
1070
1075
1080
(m) [Pd_6**1***$_8$(OTf)$_5$(NO_3)]$^{6+}$
theoretical
[Pd_6**1***$_8$(OTf)$_6$]$^{6+}$
360 min
180 min
120 min
60 min
30 min
10 min
5 min
1205
1210
1215
1220
(n) [Pd_2**1***$_3$(OTf)$_2$]$^{2+}$
theoretical
360 min
180 min
120 min
60 min
30 min
10 min
5 min
1340

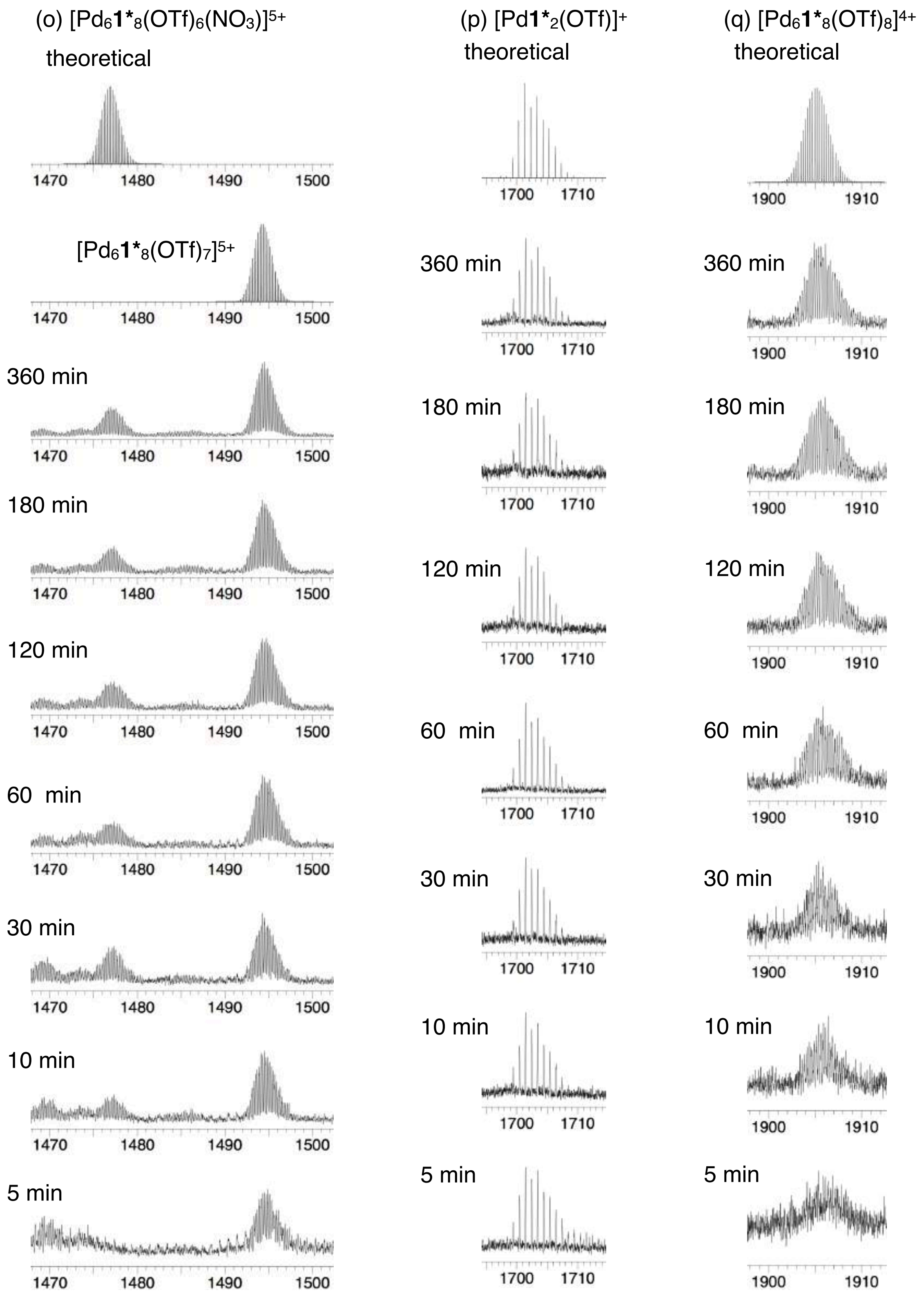
(o) [Pd6 1*8(OTf)6(NO3)]5+
theoretical
[Pd6 1*8(OTf)7]5+
360 min
180 min
120 min
60 min
30 min
10 min
5 min
1470 1480 1490 1500
(p) [Pd1*2(OTf)]+
theoretical
360 min
180 min
120 min
60 min
30 min
10 min
5 min
1700 1710
(q) [Pd6 1*8(OTf)8]4+
theoretical
360 min
180 min
120 min
60 min
30 min
10 min
5 min
1900 1910

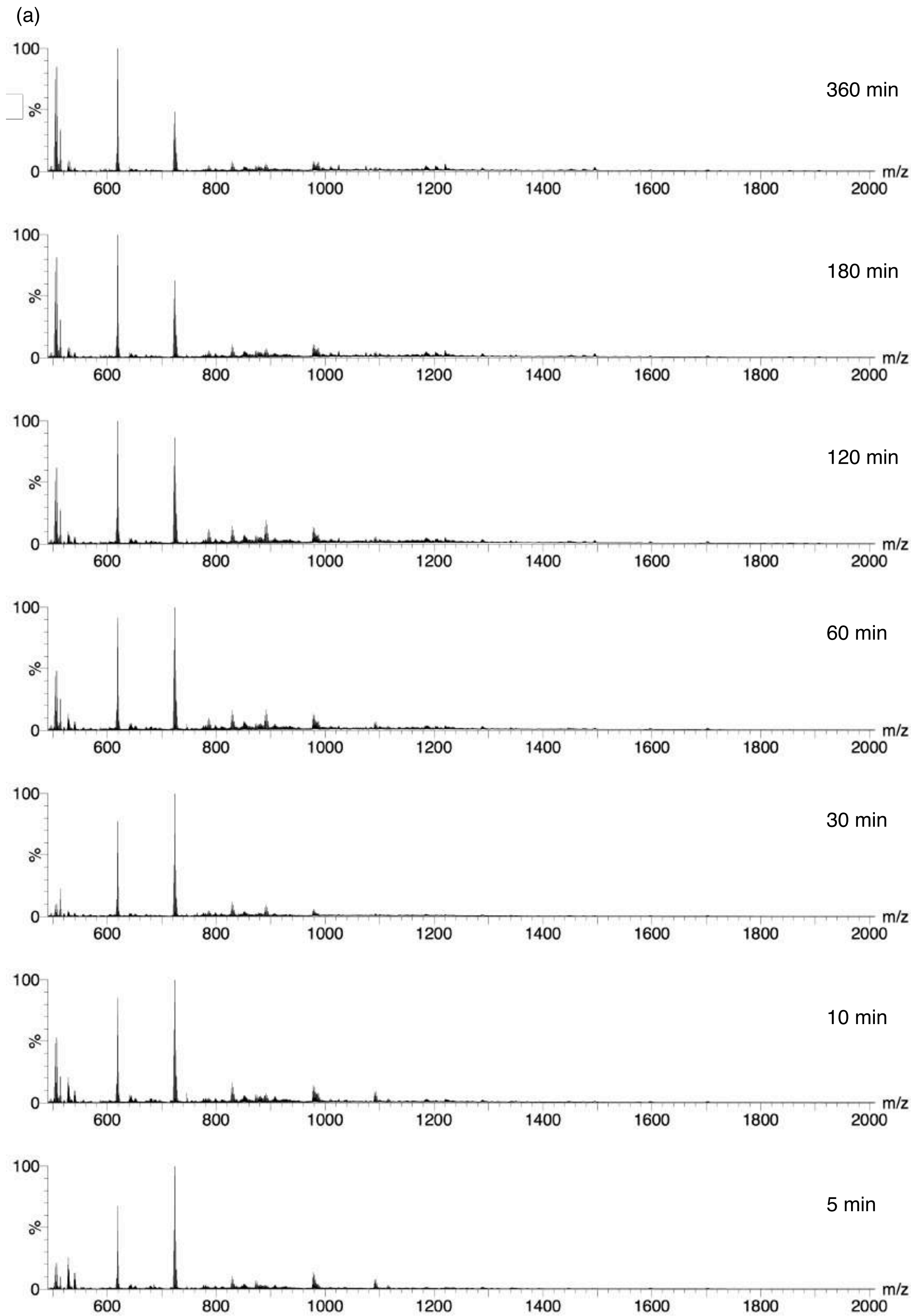

Figure S3. (a) Time-dependent ESI-TOF mass spectra of the reaction mixture for the self-assembly of the $Pd_6\mathbf{1}_8(OTf)_{12}$ capsule from racemic **1** and $PdPy^*_4(OTf)_2$. (b) Magnified ESI-TOF mass spectra of (a) (*m*/*z* 500–1300). (c) Magnified ESI-TOF mass spectra of (a) (*m*/*z* 1300–2000). (d)–(n) Magnified ESI-TOF mass spectra for the region of $[Pd\mathbf{1}Py^*_2]^{2+}$ (d); $[\mathbf{1}\cdot H_2 - COPy]^+$ and $[\mathbf{1}\cdot H - COPy]^+$ (e); $[\mathbf{1}\cdot H]^+$ (f); $[Pd\mathbf{1}(OTf)]^+$ and $[Pd_2\mathbf{1}_2(OTf)_2]^{2+}$ (g); $[Pd_6\mathbf{1}_8(OTf)_5]^{7+}$ (h); $[Pd_3\mathbf{1}_8Py^*_3]^{6+}$ (i); $[Pd\mathbf{1}Py^*(OTf)]^+$ (j); $[Pd_6\mathbf{1}_8(OTf)_6]^{6+}$ (k); $[Pd_2\mathbf{1}_3(OTf)_2]^{2+}$ (l); $[Pd_6\mathbf{1}_8(OTf)_7]^{5+}$ (m); $[Pd\mathbf{1}_2(OTf)]^+$ (n).

(b)

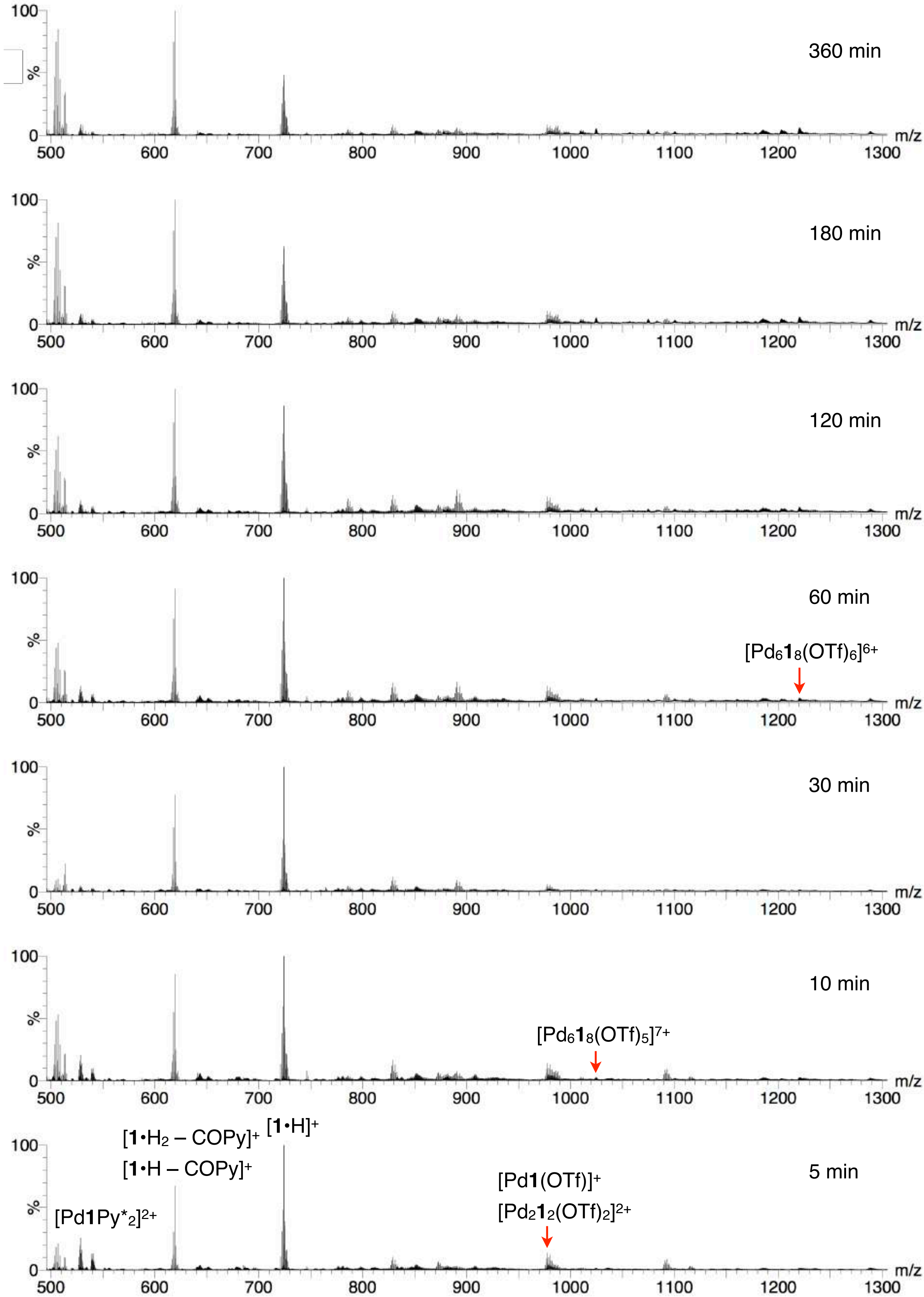

100
%
0
500
600
700
800
900
1000
1100
1200
1300
m/z
360 min
180 min
120 min
60 min
[Pd₆1₈(OTf)₆]6+
30 min
10 min
[Pd₆1₈(OTf)₅]7+
5 min
[1•H₂ – COPy]+
[1•H – COPy]+
[1•H]+
[Pd1Py*₂]2+
[Pd1(OTf)]+
[Pd₂1₂(OTf)₂]2+

(c)

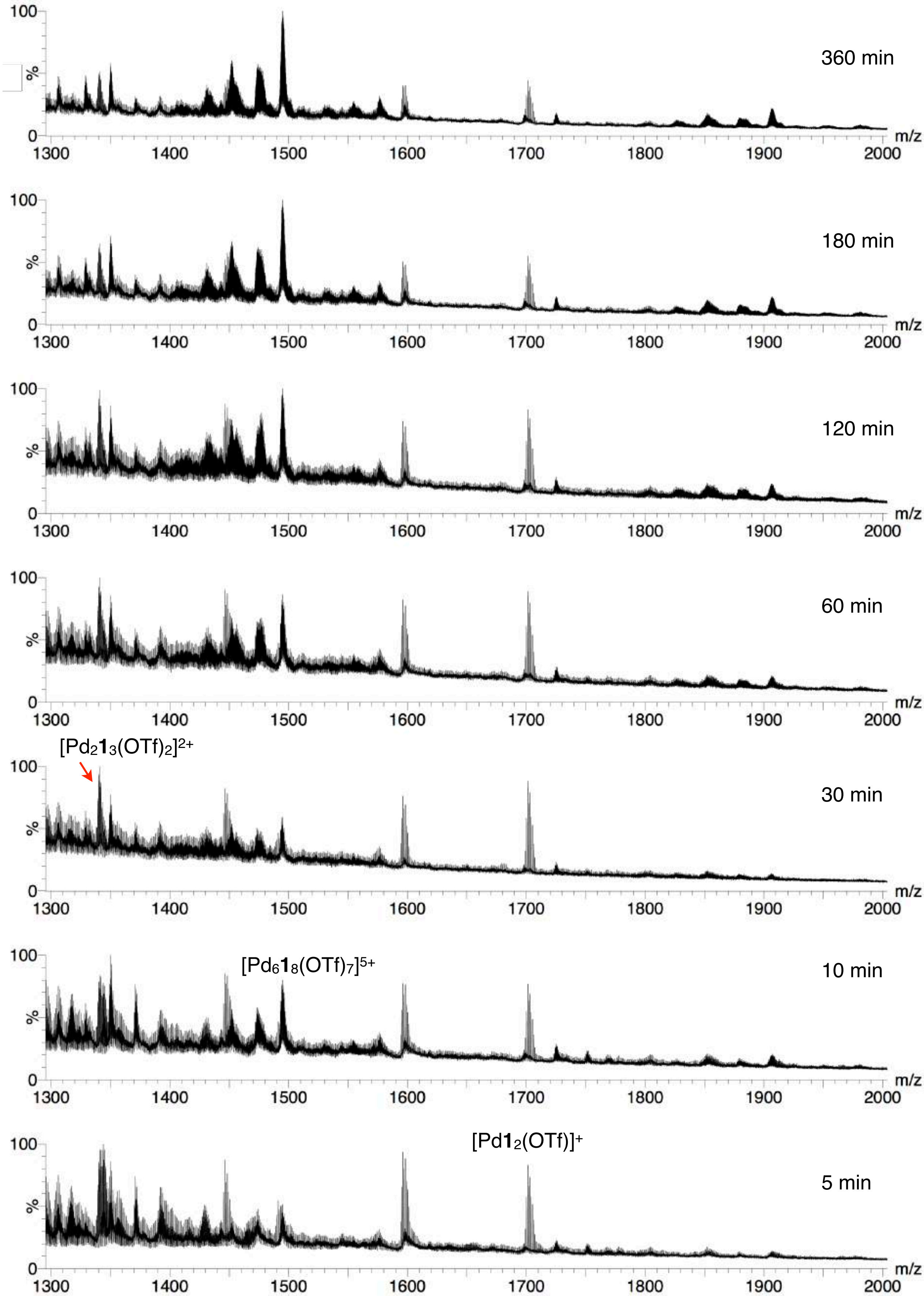

360 min
180 min
120 min
60 min
30 min
10 min
5 min
[Pd21 3(OTf)2]2+
[Pd61 8(OTf)7]5+
[Pd1 2(OTf)]+
m/z
%

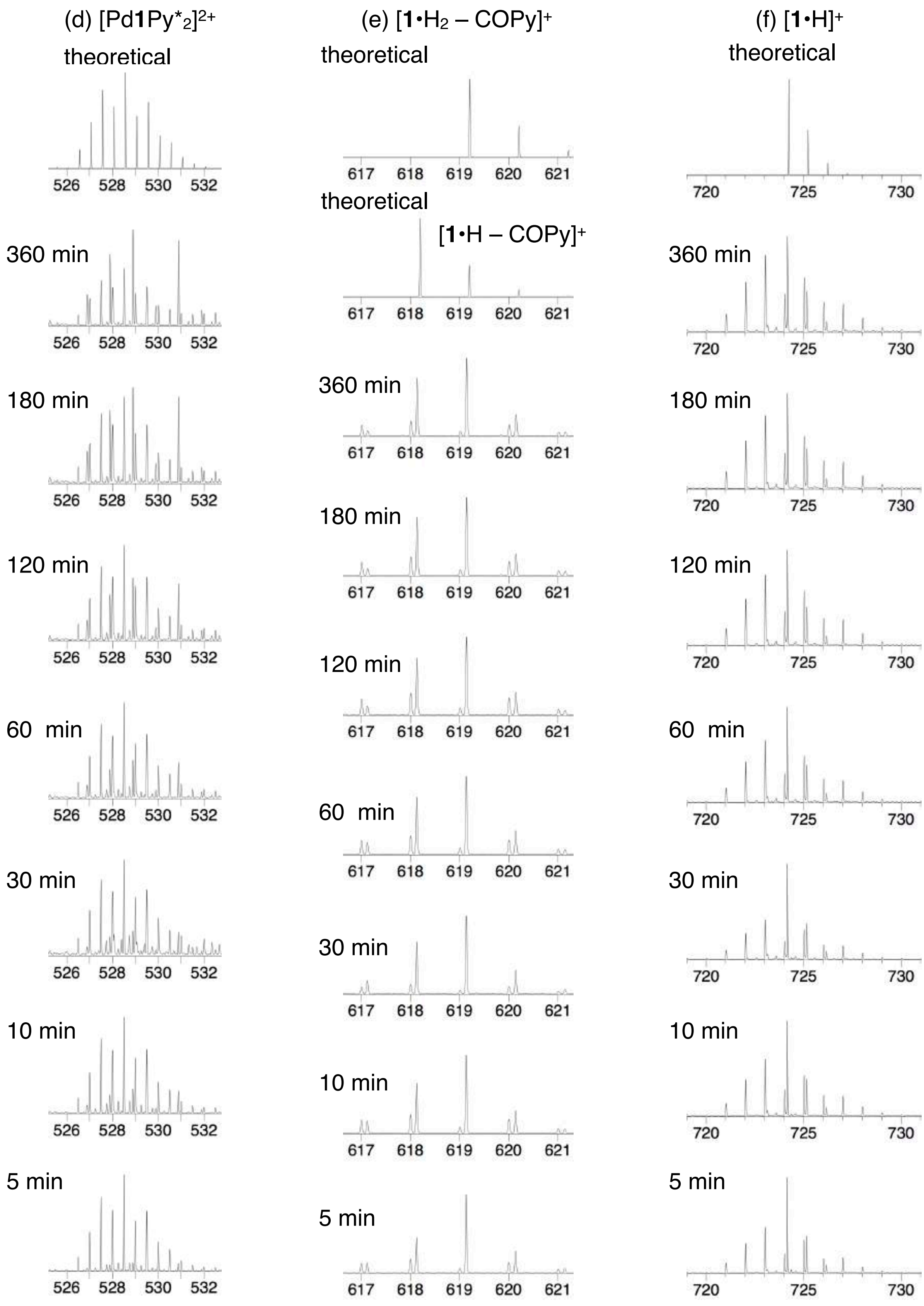
(d) [Pd1Py*2]2+
(e) [1•H2 – COPy]+
(f) [1•H]+
theoretical
theoretical
[1•H – COPy]+
360 min
180 min
120 min
60 min
30 min
10 min
5 min
526
528
530
532
617
618
619
620
621
720
725
730

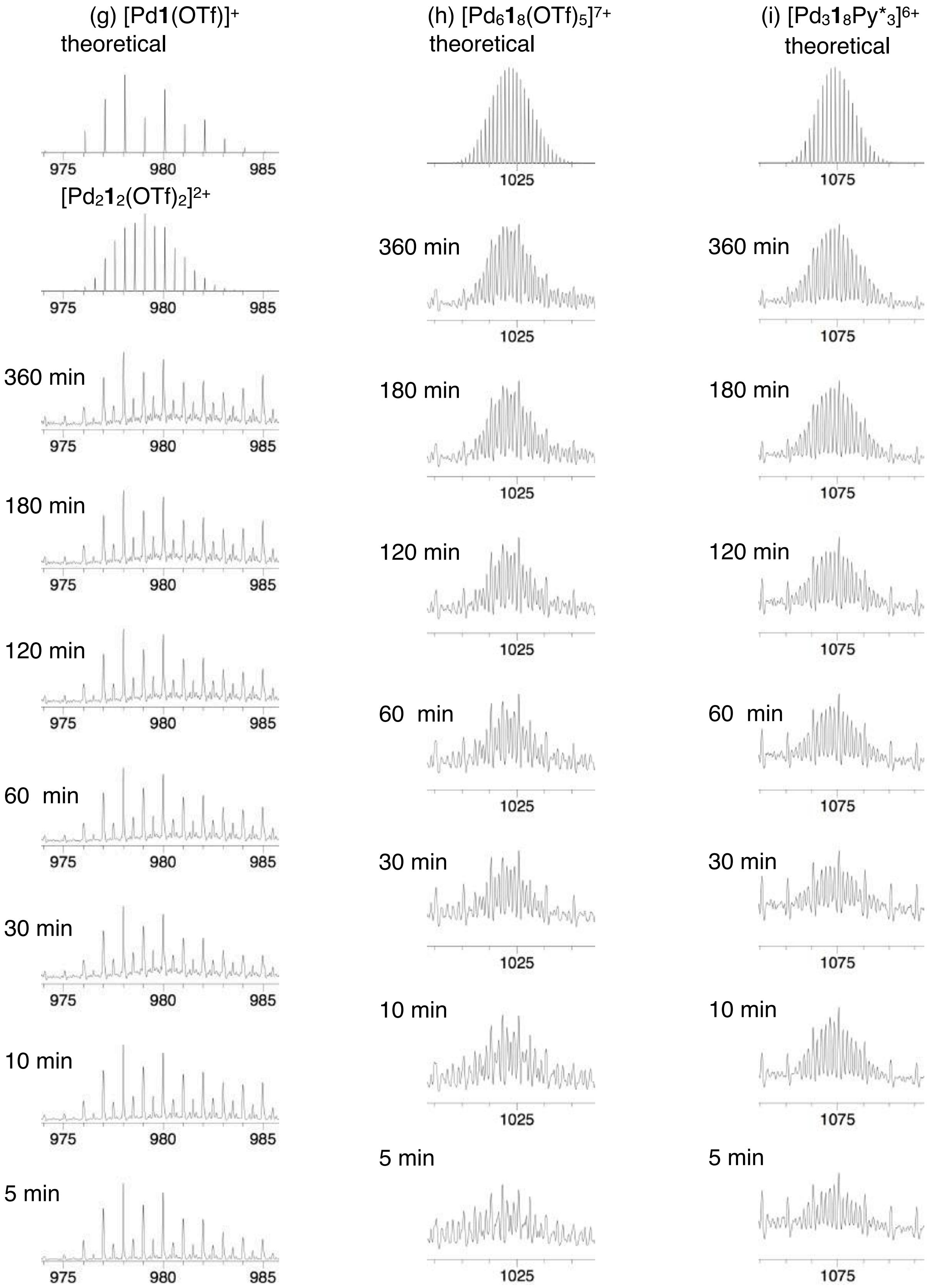
(g) [Pd1(OTf)]+
theoretical
975
980
985
[Pd21 2(OTf)2]2+
360 min
180 min
120 min
60 min
30 min
10 min
5 min
(h) [Pd61 8(OTf)5]7+
theoretical
1025
(i) [Pd31 8Py*3]6+
theoretical
1075

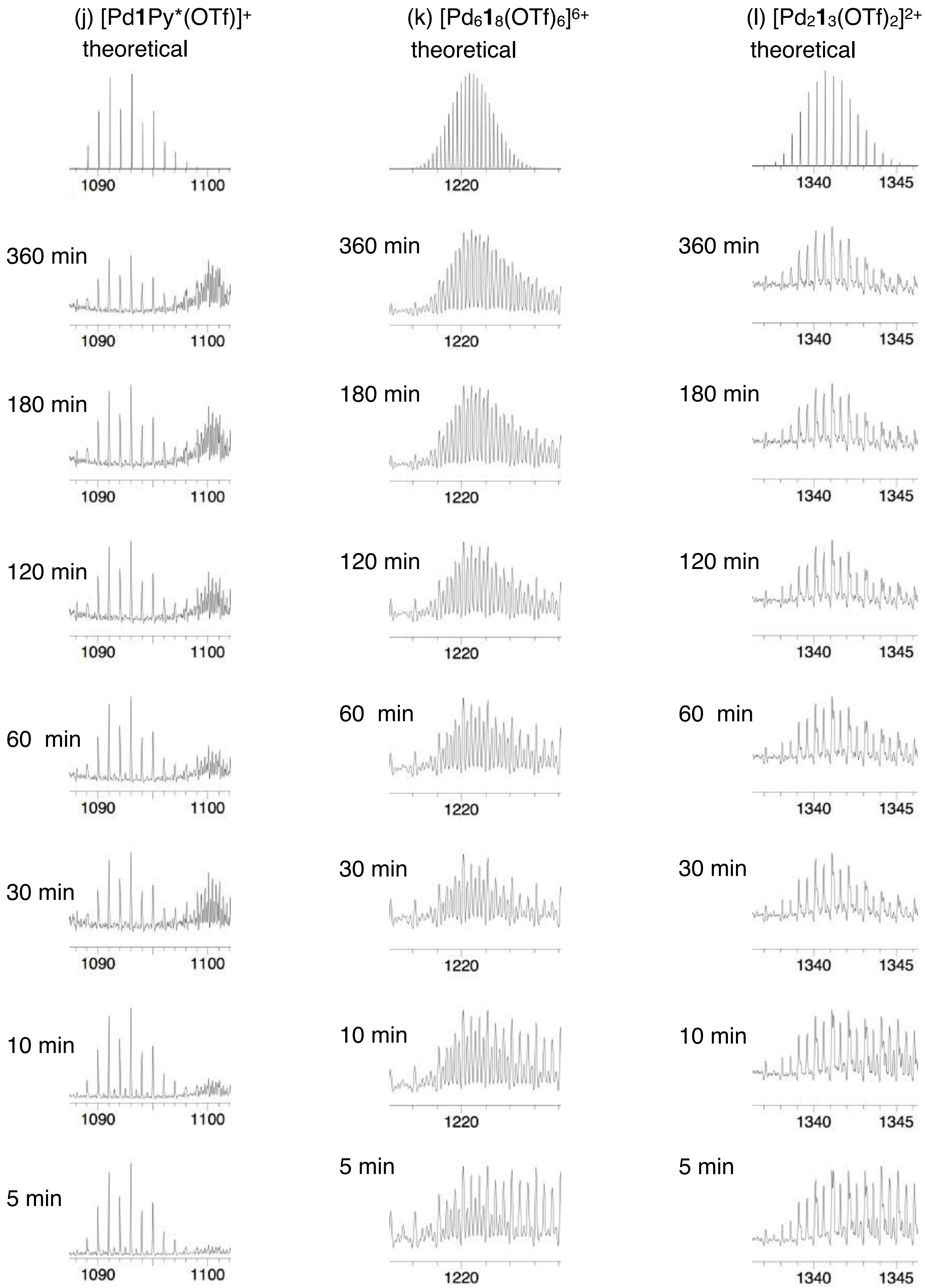
(j) [Pd1Py*(OTf)]+
theoretical
(k) [Pd618(OTf)6]6+
theoretical
(l) [Pd213(OTf)2]2+
theoretical
360 min
180 min
120 min
60 min
30 min
10 min
5 min
1090
1100
1220
1340
1345

(m) $[Pd_6\mathbf{1}_8(OTf)_7]^{5+}$

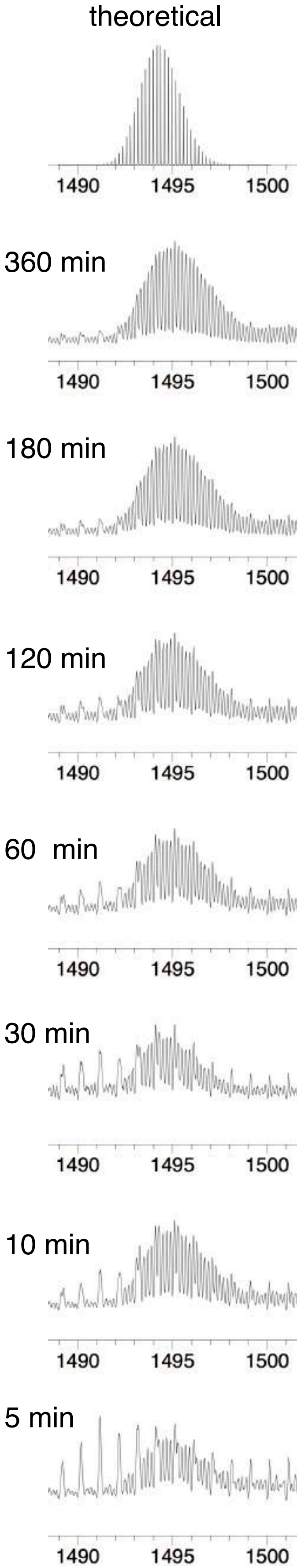

(n) $[Pd\mathbf{1}_2(OTf)]^{+}$

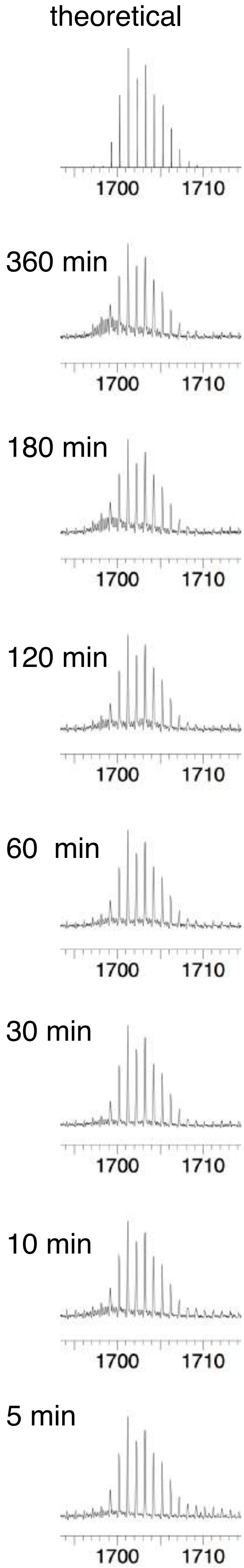

References

[1] M. J. Hardie, C. J. Sumby, *Inorg. Chem.* **2004**, *43*, 6872–6874.

[2] V. E. Pritchard, D. R. Martir, S. Oldknow, S. Kai, S. Hiraoka, N. J. Cookson, E. Zysman-Colman, M. J. Hardie, *Chem. Eur. J.* **2017**, *23*, 6290–6294.